Numerical modelling of hydrodynamics and tidal energy extraction in the Alderney Race: a review

Thiebot, Jerome; Coles, Daniel; Bennis, Anne-Claire; Guillou, Nicolas; Neill, Simon; Guillou, Sylvain; Piggott, Matthew

Philosophical Transactions of the Royal Society A: Mathematical, Physical and Engineering Sciences

DOI:
10.1098/rsta.2019.0498

Published: 21/08/2020

Peer reviewed version

PHILOSOPHICAL TRANSACTIONS
OF THE ROYAL SOCIETY A
MATHEMATICAL, PHYSICAL AND ENGINEERING SCIENCES

Numerical modelling of hydrodynamics and tidal energy extraction in the Alderney Race: a review

Journal:	*Philosophical Transactions A*
Manuscript ID	RSTA-2019-0498.R1
Article Type:	Review
Date Submitted by the Author:	n/a
Complete List of Authors:	Thiébot, Jérôme ; UNICAEN, Coles, Daniel; University of Southampton, Bennis, Anne-Claire; Université de Caen Normandie, Laboratoire de Morphodynamique Continentale et Côtière Guillou, Nicolas; CEREMA Direction territoriale Ouest et Direction technique Eau mer et fleuves, Laboratory of Coastal Engineering and Environment Neill, Simon; Bangor University, School of Ocean Sciences Guillou, Sylvain; UNICAEN Piggott, Matthew; Imperial College London, Earth Science and Engineering
Issue Code (this should have already been entered and appear below the blue box, but please contact the Editorial Office if it is not present):	ALDERNEY
Subject:	Computer modelling and simulation < COMPUTER SCIENCE, Oceanography < EARTH SCIENCES, Environmental engineering < ENGINEERING AND TECHNOLOGY, Energy < ENGINEERING AND TECHNOLOGY, Ocean engineering < ENGINEERING AND TECHNOLOGY, Power and energy systems < ENGINEERING AND TECHNOLOGY
Keywords:	Alderney Race, Raz Blanchard, Resource, Tidal turbine

Author-supplied statements

Relevant information will appear here if provided.

Ethics

Does your article include research that required ethical approval or permits?:
This article does not present research with ethical considerations

Statement (if applicable):
CUST_IF_YES_ETHICS :No data available.

Data

It is a condition of publication that data, code and materials supporting your paper are made publicly available. Does your paper present new data?:
My paper has no data

Statement (if applicable):
CUST_IF_YES_DATA :No data available.

Conflict of interest

I/We declare we have no competing interests

Statement (if applicable):
CUST_STATE_CONFLICT :No data available.

Authors' contributions

This paper has multiple authors and our individual contributions were as below

Statement (if applicable):
As this article is a review, the authorsâ€™ contribution consisted in concepting and designing the article and in revising it critically. The authorsâ€™ contributions were shared in the following way: the â€˜hydrodynamic characterisation and assessment of the AEPâ€™ section was mainly written by DC, JT, SN, NG, MP and SG. The main contributors to the â€˜Ambient turbulence and waves climatesâ€™ section are ACB, JT and SG. The â€˜Impacts of the tidal turbines on the physical conditionsâ€™ section has been principally written by JT, SN, and NG. The â€˜Array design testing and optimisationâ€™ section has been written mainly by DC, MP, JT and SN. All authors approved the manuscript.

PHILOSOPHICAL TRANSACTIONS A

Phil. Trans. R. Soc. A.
doi:10.1098/not yet assigned

Numerical modelling of hydrodynamics and tidal energy extraction in the Alderney Race: a review

Jérôme Thiébot[1], Daniel Coles[2,3], Anne-Claire Bennis[4], Nicolas Guillou[5], Simon Neill[6], Sylvain Guillou[1] and Matthew Piggott[7]

1. Normandie University, UNICAEN, LUSAC, EA4253, Cherbourg, France
2. Energy and Climate Change Division, Sustainable Energy Research Group, School of Engineering, University of Southampton, United-Kingdom
3. SIMEC Atlantis Energy, 4th Floor, Edinburgh Quay 2, 139 Fountainbridge, Edinburgh, EH3 9QG, United Kingdom
4. Normandie University, UNICAEN, CNRS, UNIROUEN, M2C, Caen, France
5. Laboratoire de Génie Côtier et Environnement (LGCE), Cerema, Direction Eau Mer et Fleuves, ER, Plouzané, France
6. School of Ocean Sciences, Bangor University, Menai Bridge, United-Kingdom
7. Department of Earth Science and Engineering, Imperial College London, London, United-Kingdom

Keywords: Alderney Race, Raz Blanchard, Resource, Tidal turbine

*Author for correspondence (jerome.thiebot@unicaen.fr).
†Present address: LUSAC, UNICAEN, 60 rue Max Pol Fouchet, Cherbourg-en-Cotentin, 50130, France

Abstract

The tides are a predictable, renewable, source of energy that if harnessed, can provide significant levels of electricity generation. Alderney Race, with current speeds that exceed 5 m/s during spring tides, is one of the most concentrated regions of tidal energy in the world, with the upper bound resource estimated at 5.1 GW. Due to its significance, the Alderney Race is frequently used for model case studies of tidal energy conversion, and here we review these model applications and outcomes. We examine a range of temporal and spatial modelling scales, from regional models applied to resource assessment and characterisation, to more detailed models that include energy extraction and array optimization. We also examine a range of physical processes that influence the tidal energy resource, including the role of waves and turbulence in tidal energy resource assessment and loadings on turbines. The review discusses model validation, and covers a range of numerical modelling approaches, from two-dimensional to three-dimensional tidal models, two-way coupled wave-tide models, Large Eddy Simulation (LES) models, and the application of optimization techniques. The review contains guidance on model approaches and sources of data that can be used for future studies of the Alderney Race, or translated to other tidal energy regions.

1. Introduction

With increasing energy demand and a need to reduce greenhouse gas emissions, the share of renewable energy in the global energy mix is constantly increasing. Among the different renewable technologies, the exploitation of coastal currents by tidal kinetic energy converters has the dual advantages of predictability (which facilitates integration into electricity networks) and limited visual impact (which eases acceptance by local coastal communities). At the time of writing, this technology is still under development, with several test/demonstration projects now built and operational and further development ongoing in preparation for industrial rollout.

With peak spring tide velocities exceeding 5 m/s [1], the Alderney Race (AR), which extends over 15 km from the Alderney Island (Channel Islands) to Cap de la Hague (France), is one of the most promising tidal energy sites in the world. Interest in developing tidal stream projects in AR has been shown by developers such as OpenHydro, Alstom and SIMEC Atlantis Energy. The French government has also developed subsidy support through a 150 Euro/MWh Feed In Tariff (FIT) for 'marine hydraulic energy' that includes tidal range, tidal stream and wave technologies [2]. Today (in 2020), extensive field campaigns and modelling studies have characterised the resource of the AR, but no turbines have yet been tested on site because pilot tidal farm projects have been delayed. Projects that were in the early stages of development have been abandoned because investments in both the OpenHydro and the Alstom turbines have ceased (which impacted the Nepthyd and the Normandie Hydro projects in French territorial waters and the joint venture between Alderney Renewable Energy and OpenHydro in Alderney territorial waters) [3]. However, as tidal energy technology matures, new projects are expected. For instance, SIMEC Atlantis Energy endeavours to build a demonstration tidal array in the AR in 2021 and to increase the capacity of this project from 2022 [4]. Hydroquest and CMN (Constructions Mécaniques de Normandie) also plan to install a pilot farm in the AR [5].

Thanks to the scientific and industrial interest in the AR, there is an extensive body of literature on this site, with most studies relying on numerical modelling. An extensive review of these different studies is therefore a unique opportunity to provide potential developers with key information about the state-of-the-art in numerical approaches currently considered (at different spatial and temporal scales) to characterise the tidal stream energy resource and optimise the design and location of single turbines and/or turbine arrays.

The application of numerical models has become essential in the early phases of tidal energy projects because the models can address a number of important questions and issues. In this review article, four main issues are considered. Firstly, regional models that simulate tidal propagation can be used to map the hydrodynamic characteristics of a given site, which provides vital information in selecting optimal locations to deploy turbines. Hydrodynamic models are also useful for assessing the turbine loading resulting from the combined effects of tidal current, waves and turbulence, which is essential for turbine design. This is the subject of section 2, in which we review, discuss and compare different methodologies for simulating the hydrodynamics of the AR as well as on-going work on waves and turbulence. Secondly, hydrodynamic models are also useful to evaluate the technically exploitable production (generally expressed as an Annual Energy Production, hereinafter AEP). Studies dedicated to the assessment of the AEP are presented in section 3. Thirdly, simulations including the effects of turbines on the underlying hydrodynamics enable the impact of tidal energy extraction on the wider environment to be assessed, and interactions between devices through their wakes to be accounted for. This opens up the potential to quantify device-device and site-site interactions, including the modification of the tidal resource due to energy extraction. Existing studies that simulate energy extraction in the AR and their impact on the physical conditions are presented in section 4. Finally, section 5 is dedicated to the results of array design testing and layout optimisation in the AR.

2. Hydrodynamic characterisation

In the early stages of tidal energy projects, numerical models can be used to identify and contrast potential sites for tidal energy extraction (site screening). Once a site has been identified, numerical models are used to characterise in more detail the hydrodynamics, focusing on flow characteristics that are important for the selection and design of turbines and arrays, such as the spatial distribution of mean/peak current speeds, the associated power density, the tidal flow asymmetry, and the rectilinearity of the flow. Once turbine characteristics have been selected (e.g. design features such as rotor diameter, rated power and hub height and performance characteristics such as power coefficient), the AEP can be estimated, based upon a proposed scenario of turbine deployment and array layout (which is the subject of section 3).

Legrand [6] and IEC [7] provide recommendations on the way to assess the resource (encompassing the hydrodynamic characterisation and the AEP assessment) from both in-situ measurements and numerical models. The objectives of the IEC specification are to provide a methodology that can be applied across different sites, to ensure accuracy in the resource estimation and to provide a consistent way to report the results. As regards the use of numerical models, the specification provides guidance on the ways in which models should be applied depending on the stage of the project development. While a certain level of uncertainty is permitted for site screening or feasibility studies, highly reliable models are required for the more advanced stages of turbine/array design. The modelling objectives thus have important implications on the choice of the model settings, the calibration/validation procedure, and the presentation of the results. In this section, we review modelling studies dedicated to the hydrodynamic characterisation of the AR. We begin our review by appraising large-scale (continental shelf scale) studies (section 2a) and regional hydrodynamic characterisation (section 2b). The main characteristics of the hydrodynamic models reviewed in sections 2a and 2b are synthesized in Table 1. Afterwards, we present investigations dedicated to turbulence and wave characterisation (section 2c and 2d, respectively).

References	Model	Studied zone / Minimum cell size	Forcing	Data used for the model calibration/ validation	Objectives
DTI [8]	POLCOMS (FD)	1.8 km	Not mentioned	Not mentioned	Resource assessment (intercomparison of sites)
SHOM [9]	HYCOM3D (FD)	1.8 km	Operational Mercator global ocean analysis and forecast system + wind + atmospheric pressure	Not mentioned	Resource assessment (intercomparison of sites)
Robins et al. [10]	ROMS3D (FD)	NW European continental shelf / 1 km	10 constituents (TPXO7)	Tidal gauges (20 stations) + Current meters (15 stations)	Resource assessment (intercomparison of sites)

Campbell et al. [11]	MARS2D (FD)	Coasts of France / 250 m	115 constituents cstFRANCE) + wind + atmospheric pressure	Tidal gauges (19 stations)	Resource assessment (intercomparison of sites)
Guillou et al. [12]	Harmonic database built from MARS2D (FD) predictions	Coasts of France / 250 m	115 constituents (cstFRANCE) + wind + atmospheric pressure	Tidal gauges (18 stations) + Current meters (40 stations)	Resource assessment (intercomparison of sites)
Bailly du Bois et al. [13]	MARS2D (FD)	NW European continental shelf / 110 m	10 constituents (FES2004) + wind + atmospheric pressure	Current meters (11 stations) + Tidal gauges (3 stations) + Tracer releases + Drifter tracking	Dispersion of solute tracers
Thiébaut et al. [14]	MARS2D (FD)	NW European continental shelf / 110 m	14 constituents FES2012	Same as Bailly du Bois et al. (2012) + Towed and bottom-mounted current meters	Resource assessment
Pal et al. [15]	ADCIRC (FE)	English Channel / min. cell size not mentioned	8 constituents	Not mentioned	Resource assessment
Blunden et al. [16]	Telemac2D (FE)	English Channel /1 km	Tidal constituents interpolated between two harbours	Tidal gauges (14 stations)	Resource assessment (model validation)
Neill et al. [17]	POLCOMS3D (FD)	Alderney Race and surrounding waters / 500 m	2 constituents [18]	Tidal gauges (3 stations) + Admiralty tidal diamonds (4 stations)	Effect of the tidal energy extraction
Coles et al. [1]	Telemac2D (FE)	English Channel / 250 m	9 constituents	Tidal gauges (13 stations) + Current meters (3 stations)	Resource assessment + Effect of the tidal energy extraction
Bennis et al. [19]	MARS3D (FD) coupled to WaveWatch-III	Western part of the English Channel / 120 m	115 tidal constituents (cstFRANCE) + Waves + Winds	Tidal gauges (2 stations) + ADCP (waves and currents) at 1 station	Interactions between waves and current
Thiébot et al. [20]	Telemac3D (FE)	English Channel / 100 m	11 constituents TPXO8	Current meters (5 stations)	Wake-field study

Table 1: Main characteristics of the hydrodynamic models of the AR. The references are sorted by scale (large-scale models and then regional models) and by spatial resolution. The data in the 5th column is generally acquired and applied more broadly than just within the AR. In the "Model" column, FE and FD

stand for Finite Element and Finite Difference, respectively. Telemac (2D or 3D) and ADCIRC models use unstructured meshes. Other models use structured meshes.

a. Large-scale studies

Site screening and feasibility studies generally rely on models that simulate tidal propagation over relatively large domains (e.g. the European shelf) with relatively coarse mesh resolution (minimum cell size of the order 1 km). Rather than providing a detailed hydrodynamic characterisation of a particular tidal energy site, these models provide data that can be used to understand the general characteristics of the tide in regions that encompass one or more tidal energy sites. Examples of large-scale models that include the AR are the 3D (three-dimensional) POLCOMS [8] and ROMS [10] configurations which covers the NW European shelf. There are also the HYCOM3D configuration of the SHOM (French Navy) [9] and the MARS2D configuration of the Previmer project [11, 12] that both cover the English Channel and the Bay of Biscay. The model of Robins et al. [10] was mainly used to contrast the tidal resource of several tidal stream energy sites across the NW European shelf (Figure 1a), focusing in particular on the interactions between the main tidal constituents. Hence, the spring-neap ratio, calculated from the magnitude of the current generated by the M_2 and S_2 tidal constituents, indicated that the variability between spring and neap flow is relatively low in the AR, compared to other sites in the NW European shelf seas. This implies a limited variation of electricity production over lunar timescale, which would facilitate the integration of the energy into the electrical network. To quantify the gain due to this low variability of the current magnitude over lunar timescale, Robins et al. [10] compared the total annual power produced at two sites having a similar mean peak spring velocities, one in the AR and one in the Pentland Firth (separating mainland Scotland from the Orkney Islands), and showed that the total annual power is 10 % greater in the AR. Robins et al. [10] also investigated the daily modulation of the tide, focusing on the M_2, S_2, K_1 and O_1 tidal constituents, which revealed that the tide in the AR is strongly semi-diurnal. They also investigated the tidal asymmetry induced by the relationship between the M_2 and the M_4 tidal constituents and showed that the spatial distribution of the tidal asymmetry is particularly complex around the Channel Islands, which implies that high resolution models should be used in this area for a detailed hydrodynamic characterisation. Campbell et al. [11] also used a large-scale model to compare the resource of several tidal energy sites including the AR. Their analysis, restricted to sites located along the coasts of France, relied on the output of a depth-averaged configuration of MARS2D (Previmer project). Complementary to [10], they focused on the current magnitude and the extractable power (rather than on the characteristics of the tidal constituents and their mutual interactions) and identified twenty potential tidal energy sites along the coast of France, confirming that the AR has the greatest resource. They provided several maps of mean current speed and power density, and identified a zone of particular interest in the AR wherein currents exceeds 2.5 m/s 40% of the time and where the mean ebb/flow misalignment is low. Finally, they provided estimates of extractable power, considering different scenarios of tidal energy extraction (different turbine densities and performances), which will be discussed in section 3. Guillou et al. [12] also investigated the tidal resource along the coast of France and highlighted the significant potential of the AR. Their analysis relied on a tidal current harmonic database built from the results of a MARS2D configuration (Previmer project) (Figure 1b). In addition to the results of Campbell et al. [11], they included a validation of current predictions, utilising Acoustic Doppler Current Profiler (hereinafter ADCP) measurements acquired near the AR by Bailly du Bois et al. [13]. Similarly to Robins et al. [10], they analysed the effects of the interactions between the major tidal constituents on both the variability of the resource over a spring-neap cycle and the current asymmetry. Not only were their results consistent with [10] on the spring-neap tidal variability and the semi-diurnal asymmetry, but the improved spatial resolution of their model (250 m compared with 1 km)

permitted detailed maps of the AR to be developed, representing the spatial distribution of peak current speed, power density, rectilinearity of the flow and metrics of the temporal variability of tidal currents. These detailed cartographies exhibited the important total exploitable area of the AR and also provided further insights into tidal currents asymmetry at the scale of straits and in the vicinity of islands and headlands. The region off the Cotentin Peninsula exhibited weak tidal asymmetry, which in conjunction with reduced spring-neap variability, resulted in more attractive energy conversion.

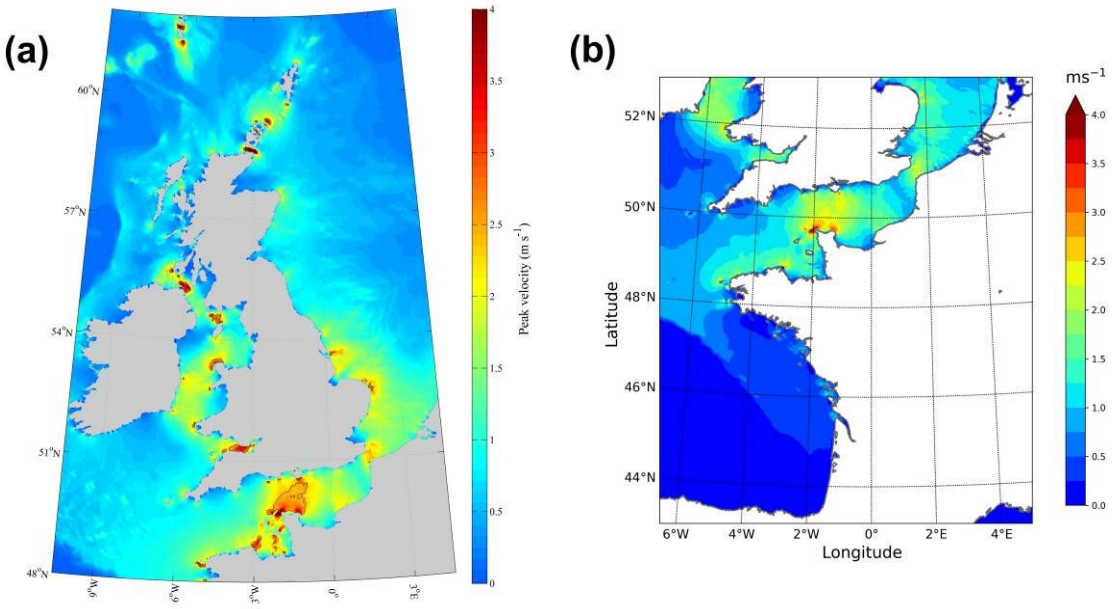

Figure 1: Spatial coverage of the models of (a) [10] and (b) [12]. The colour represents the maximum depth-averaged tidal velocity magnitude. The velocities have been computed from the (a) M_2, S_2, K_1, O_1 and M_4 constituents and (b) M_2, S_2, N_2, K_2, K_1, O_1, P_1, Q_1, M_4 and MS_4 constituents. Figure 1a was reprinted from [10] Robins et al. (2015) Characterising the spatial and temporal variability of the tidal-stream energy resource over the northwest European shelf seas. Applied Energy, Vol. 147, pp. 510-522. Copyright 2020, with permission from Elsevier. Figure 1b was adapted from [12] Guillou et al. (2018) Characterising the tidal stream power resource around France using a high-resolution harmonic database. Renewable Energy, Vol. 123, pp. 706-718. Copyright 2020, with permission from Elsevier.

b. Regional scale studies

Complementary to the large-scale models described above, a series of higher resolution model studies were conducted specifically on the AR. For instance, Bailly du Bois et al. [13] set up a configuration of the depth-averaged MARS2D model to simulate the hydrodynamics of this site. Their model configuration was initially designed to analyse the dispersion of solute substances in the AR (controlled releases of tritium carried out by the Orano nuclear recycling plant) and has subsequently been used in several tidal resource investigations [21, 14]. This model has been validated using a large number of data acquired around the Cap de la Hague, including ADCP and tidal gauge measurements, Lagrangian drifter tracks, and concentration of tracer (releases of tritium). It is noteworthy that these datasets are accessible online [13] and enable a preliminary calibration/validation for models of the AR. For instance, the ADCP data of [13] were used to validate the models of Thiébot et al. [22] and Guillou et al. [12]. Unfortunately, the available ADCP time-series are short (time-series of 24 h) and the ADCPs were deployed several kilometres from the zone of peak current speed. Therefore, for a detailed resource characterisation, this dataset should be complemented with additional measurements acquired in the

area where the turbines would be deployed. Hence, Thiébaut et al. [14] benefitted from new data acquisition in the AR [23, 19] that enabled a refinement of the model of Bailly du Bois et al. [13]. In particular, the comparison of model predictions to towed and bottom-mounted ADCP measurements revealed that the model configuration of Bailly du Bois et al. [13] tended to overestimate the current velocity magnitude (+20% during ebb tide and +11% during flood tide). By constraining the model predictions using the velocity measurements, they obtained a significant improvement in model performance, and the overestimation of the velocities was reduced by a factor of two. Blunden and Bahaj [16] also proposed a resource assessment of the AR, relying on a 2D (two-dimensional) model (Telemac2D). A new Telemac2D model with a 1 km resolution was built by Coles et al. [1] who assessed the resource of the tidal sites located around the Channel Islands (including the AR). Their model covered the English Channel with a minimum cell size of 250 m. The surface elevation acquired at 13 tidal gauges in the English Channel were compared to the model results to compute the amplitude and phase errors for the M_2 and S_2 tidal constituents, with good agreement demonstrated. The model validation also relied on ADCP data acquired in the western part of the AR (three ADCPs each deployed for more than 30 days) and relied on the M_2 and S_2 tidal ellipses (major axis amplitude and phase and inclination). As regards the M_2 constituent, they obtained differences (i) smaller than 10% for the amplitude of the major axis (+10%, +4% and -5% depending on the ADCP), (ii) of the order of 5° accuracy for the phase and (iii) of the order of 10°accuracy for the inclination of the tidal ellipse. Coles et al. [1] thus confirmed that a 2D model could satisfactorily simulate the propagation of the major tidal constituents in the AR. Once the model was validated, they investigated the spatial distribution of the power density and then assessed the exploitable tidal resource with the upper bound for power extraction (which is described in section 3). A model configuration of the AR was also proposed by Neill et al. [17]. This model relied on the 3D solver POLCOMS and was designed mainly for assessing the effect of tidal turbines on the dynamics of sandbanks located near the island of Alderney, which is discussed in more details in section 4.

Finally, the resource of the AR was also assessed with higher resolution 3D models [19, 20]. The investigations of Thiébot et al. [20] relied on the hydrodynamic model Telemac3D forced by 11 constituents (TPXO European Shelf 2008 database, [24]). The model domain encompassed the English Channel with a resolution ranging from 10 km at offshore boundaries to 100 m within the area of interest. Meteorological and wave effects were neglected, which was justified since the ADCP data used for model validation were acquired during calm wave/meteorological conditions. The bottom roughness, which was spatially heterogeneous, was determined from sedimentary maps. In zones where the seabed was composed of rocks (as in most part of the AR), the local roughness was calibrated to obtain the best fit between the model predictions and the ADCP measurements. Five one-month long time-series of ADCP data acquired in the Alderney territorial waters were used to assess model performance. The model satisfactorily predicted the depth-averaged current magnitude (RMS errors of order 0.20 m/s), the vertical distribution of the current as well as the current velocity magnitude 15 m above the seabed, a common operating height for horizontal axis turbines (RMS errors of order 0.20 m/s) (Figure 2). This study confirmed the ability of refined models to predict the tidal current in the AR with a high degree of accuracy under calm meteorological conditions. Nevertheless, it also highlighted the difficulty in obtaining reliable power density estimates. Indeed, as the power density depends on the cubed velocity magnitude, the errors are magnified. Despite small discrepancies in velocity magnitude, Thiébot et al. [20] obtained a RMS error of order 1 kW/m^2 for the power density (Figure 2b), which remains relatively high for the estimation of the exploitable resource.

Bennis et al. [19] also used a refined 3D model to simulate the current in the AR. Complementary to Thiébot et al. [20], they focused on the other side of the Race (French territorial waters) and studied more energetic wind/wave conditions. The main goal of their study was to investigate the influence of the wind and waves on the currents. To this end, they coupled a 3D hydrodynamic solver MARS3D [25] to

the phase-averaged spectral wave model WaveWatch-III (hereafter WW-III). Their hydrodynamic model was forced by 115 tidal constituents (cstFRANCE database, [26]). In the AR, the mesh size was 120 m. Bennis et al. [19] tested and compared several model configurations to analyse the interactions between the waves, the wind and the currents (which is described in more detail in section 2d). As regards the predictions of the water elevation and the currents, they obtained good model performance with normalised RMS error (RMS error divided by the range) restricted to 0.1 for the current magnitude at different depths. Their study thus confirmed the ability of high-resolution 3D models to reliably simulate the currents over the water column in a tidal stream energy site subject to energetic meteorological conditions. It also showed that, during severe storm conditions, wind and waves significantly affected the resource.

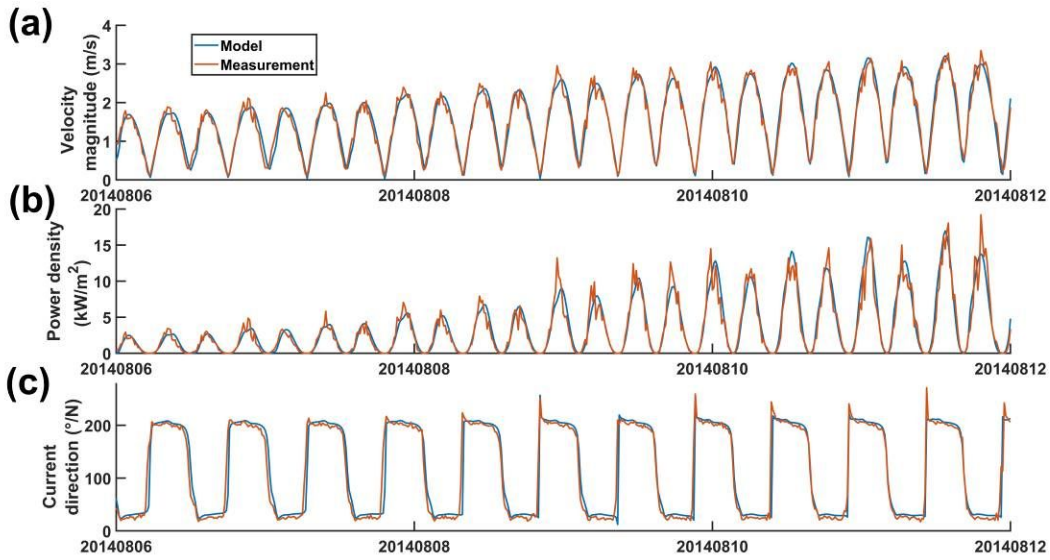

Figure 2: Time-series of horizontal current magnitude (a), power density (b) and current direction at hub height (c). The blue curve represents model predictions. The red curve represents measurements by ADCP. The time-series were extracted 15 m above the seabed. Reprinted from [20] Thiébot et al. (2020) Wake field study of tidal turbines under realistic flow conditions. Renewable Energy, ttps://doi.org/10.1016/j.renene.2019.11.129. Copyright 2020, with permission from Elsevier.

c. Turbulence characterisation

The characterisation of turbulence at tidal stream energy sites is required for two main reasons. Firstly, knowledge of turbulence characteristics is necessary to evaluate the loading conditions on the turbines, which is vital for their design. Secondly, the ambient turbulence has a strong effect on the characteristics of the wakes that form downstream of the turbines. Indeed, the greater the intensity of the background turbulence, the faster the flow recovery behind the turbines [27]. This mechanism thus has a significant influence on array design, especially in terms of the minimum distance required to ensure sufficient flow recovery between consecutive rows of turbines.

As shown in section 2b, numerous models are capable of reliably simulating tidal flows in the AR. Those models resolving time-mean flows generally rely on the unsteady (they do account for variable tidal time scales, but not the far smaller turbulent scales) Reynolds Averaged Navier-Stokes (RANS) equations and use turbulence closures. Those closures are based on a turbulent viscosity, which is either assumed to be constant [1] or is evaluated with more complex formulations such as the well-known two-equation k-ε model [10, 20, 28]. Although RANS models are well suited to simulate tidal propagation over large domains, their turbulence predictions are subject to a much greater uncertainty.

Few investigations have been conducted on the ability of RANS models to characterise turbulence at tidal stream energy sites. Nevertheless, Togneri et al. [29] highlighted interesting capabilities of the k-ε model. By comparing their model prediction to turbulence measurements in Anglesey (Wales, UK), they obtained a good agreement in terms of Turbulent Kinetic Energy (TKE), especially in the lower part of the water column (where the wave action is less important). The agreement was however poorer for turbulence dissipation. As regards the AR, different modelling strategies have been tested to simulate turbulence, including the Large Eddy Simulation, hereinafter LES, the Lagrangian-Averaged Navier-Stokes alpha model, hereinafter LANS-α, and the Leray-α model.

The concept of LES consists of filtering the Navier-Stokes equations to separate the smallest scales of motion from the others. Whereas the smallest (dissipative) scales are accounted for using subgrid-scale models, the largest scales are resolved directly (like in a Direct Numerical Simulation where all scales of motion are resolved). In comparison to the RANS approach, the LES approach captures the variable dynamics of larger eddies. In a properly configured/resolved LES set-up these eddies, which have characteristic lengths greater than the filter width, contain most of the turbulent energy and control most of the momentum transfer and turbulent mixing. The LES approach is thus a good candidate for characterising the ambient turbulence of tidal stream energy sites. In the AR, LES has been performed with a modified version of Telemac3D [30, 31] with the objective of identifying the morphological features of the seabed that trigger the formation of the largest eddies. Before applying the model to the AR, numerous developments were carried out to transform the RANS Telemac solver into a LES model. Those developments included, among others, improvements to the convection-diffusion scheme (to reduce spurious numerical dissipation), the inclusion of a synthetic eddy method (to generate incoming eddies at the boundary of the LES domain), and the implementation of subgrid-scale turbulence models. After different validation steps [32], Bourgoin [30, 31] simulated the hydrodynamics of the AR with a Telemac3D model, which captured the tidal dynamics over a 100 km x 100 km zone with a RANS approach and switched to the LES formulation in a 3 km x 3 km zone located in the AR, with minimum cell size of 5 m. Although their predictions of turbulent intensity were still underestimated (especially in the upper part of the water column), the use of LES resulted in more reliable turbulence estimates than the RANS approach. Mercier et al. [33, 34] also used LES to characterise the turbulence of the AR. Complementing [30, 31], they focused on a smaller domain and used a much finer spatial resolution (minimum cell size of 0.25 m). Their simulation relied on the Lattice Bolztmann Method (LBM), which has the advantages of minimising the numerical dissipation and enabling efficient parallelisation (which is important due to the significant computational cost associated with LES modelling). After a series of tests with increasing complexity [35], the LBM-LES model was applied to simulate the turbulence characteristics in a small area of the AR. The model predictions were compared to the measurements performed during the field campaign of the THYMOTE project by two coupled ADCPs that measured the velocity and the turbulent velocity-variance [36-38]. The results showed that the LBM-LES model was able to satisfactorily simulate the turbulence characteristics at a particular time of the tide (their study focused on the peak flood). In Mercier et al. [34], the agreement with all components of the velocity variance was remarkable. This LBM-LES model enabled insight to be gained into the dynamics of eddies that are triggered by the macro-roughnesses of the seabed (big rocks, rapid change of seabed elevation, etc). Despite the interesting capabilities of LES, it is important to keep in mind that such approach is highly constrained by its great computational cost. Indeed, a high mesh size resolution is required to obtain mesh convergence and to resolve the targeted part of the turbulence spectrum. For instance, the model of Mercier et al. [34] required 25,000h.CPU to simulate 20 minutes of tidal flow. The model of Bourgoin et al. [31], which used a coarser mesh but covered a larger domain and a longer period of time, required comparable computational resource (of the order of 100,000h.CPU). This limitation of LES prevents from approaching larger domains and longer time-scales (neap/spring tides, flood/ebb tides,

different meteorological/wave conditions…). Thus, the full characterisation of the turbulence at a site like the AR cannot be completed using LES.

LES and RANS approaches consist of modelling the turbulence (and the related transfer between the motion scales) by enhancing the fluid viscosity. An alternative approach, that is non-dissipative in nature, consists of rewriting the Navier-Stokes equations by distinguishing two types of velocities that are related with the Helmholtz operator: a Lagrangian-averaged (averaged along a particle track) velocity (referred to as the rough velocity) and an Eulerian-averaged velocity (referred to as the smooth velocity). Basically, this method consists in writing the momentum equation as an advection-diffusion equation for the rough velocity, where the advecting velocity is the smooth velocity. Two turbulence models based on this method, LANS-α and Leray-α, have been successfully applied in different fields of fluid mechanics. They have shown, in particular, their ability to simulate ocean gyres as accurately as RANS models while using double the horizontal mesh size (because they produce more eddy structure at close to the grid scale). Full details on the method and examples of oceanographic applications can be found in [39, 40]. In the AR, first tests were initiated by Adong and Bennis [21] who included the LANS-α and the Leray-α models in the ocean model MARS3D. Their results are encouraging as their model produces more turbulence than the standard RANS simulations (with a comparable grid size). However, to date, no comparison with measurements has been published, and it is therefore difficult to conclude on the effectiveness of this method for characterising the turbulence in the AR.

d. Wave characterisation

Wave characterisation at tidal energy sites is crucial for two main reasons. Firstly, the characterisation of wave climates is required to evaluate the (mean and extreme) loading conditions on the turbines. Secondly, waves are known to have a significant effect on the resource. As an example, in the Fromveur Strait (western Brittany, France), Guillou et al. [41] demonstrated that, during storm conditions (offshore significant wave height of 5 m with peak period of 14 s), the waves reduce the tidal kinetic power by 12%. The wave climates can be characterised with different types of spectral models differentiated, among other, by the code (e.g. WW-III, Tomawac or SWAN), the spatial resolution, the input data or the physical processes that are included. In this article, we distinguish two main objectives that have been pursued in studies dedicated to the AR: (objective n°1) the assessment of the wave loading on the turbines and (objective n°2) the quantification of the effect of waves on the tidal resource.

As regards the first objective, different wave models (or wave atlas) can be retained such as those presented in [42-45]. Those models have in common their long temporal coverage (which is required to compute reliable statistics, especially regarding extreme wave heights) and their validation procedure, which relies on different wave data spread out over the (large) computational domain. To illustrate the capabilities of such models, we now describe in more details the development and validation of a recent hindcast wave database [44], named HOMERE, which has been created to support the development of marine energy converters along the coasts of France facing the Atlantic and the English Channel (the AR is included in the study zone). The wave database covered the period 1994 - 2012. Wave hindcasts were performed with WW-III v4.09 [46], a spectral phase-averaged wave model. Simulations have used an unstructured mesh (10 km to 200 m spatial resolution) from open sea to the shore and have included the effects on waves of wind, tidal currents and sea level variations (computed by the MARS2D model). Numerical outputs have been validated with buoy data from the CANDHIS and Météo-France networks and altimetry data (ENVISAT, ERS1/2, TOPEX, JASON 1/2, and GFO) as well as outputs of the NOAA numerical model. The correlation coefficients between data at reference points (wave measurements or model results) and hindcasts for significant wave height and wind speed were globally good, with values greater than 90%. However, underestimations at both the higher wind speeds and the higher wave heights were observed. Those underestimations were attributed to inaccuracy of the CFSR 6-hourly wind data [47, 48] that were used to force WW-III model. The wave database of Boudière et al. [44] has then

been updated with new hindcasts and forcing fields and the period has been extended to 1994-2016 [49]. Whereas the database [44] enables the extraction of sea-states in different locations of the AR, it is worth reminding that those data should be used with care for assessing the wave loading on the turbines (objective n°1) as their wave model has not been validated with measurement data acquired in the Race (where the waves dynamics is expected to be particular due to the interaction with the strong tidal currents).

The wave model developed by Bennis et al. [19, 50] pursued a less operational objective than the model mentioned above. Indeed, Bennis et al. [19, 50] focused on theoretical aspects of the wave modelling in the presence of high current velocity magnitude, with the objective of improving understanding of the complex interactions between the wave and current fields. In contrast to the model presented in [44] which is one-way coupled (the wave model is forced by the wind, the current and the water level), the model of Bennis et al. [19] also includes the effects of the waves on the tidal current and the water level (two-way coupling) which permits, in addition to reliable predictions of sea states (objective n°1), an assessment of the influence of surface waves on the tidal resource (objective n°2). The other great advantage of this model is that it has been validated with data acquired in the AR (during the field campaign of the HYD2M project [23]). This work thus illustrates the capabilities and the limitations of the latest wave models in an area characterised by high current speeds. The approach relies on a 3D wave-current model that couples, in two-ways, the wave model WW-III and the regional circulation model MARS3D. In [19], the agreement between the model predictions and the measured data was good for significant wave height (normalised RMS = 0.08, bias = 6% and R^2 = 0.97), wave direction and frequency. As regards the wave energy spectra, they were most often bi-modal with swell and wind sea with a splitting frequency around 0.11 H_z. Numerical results were consistent with ADCP data up to a frequency twice the peak frequency of the wind sea part ($2f_w$ = 0.25 - 0.3 H_z) (Figure 3). Beyond $2f_w$, the wave energy spectra computed with local wind effects (Figure 3, blue curve) largely overestimated the wave energy in comparison to the measurements. When the local wind effect was not included in the model, there was no overestimation in this part of the spectra, but there were still significant discrepancies (Figure 3, red curve). This comparison thus shows that additional investigations are required to reduce the model uncertainties for the high frequency waves. Several possible ways could be examined such as testing a higher resolution wind forcing fields or using a more complex representation of the air-sea interactions (instead of applying a wind stress).

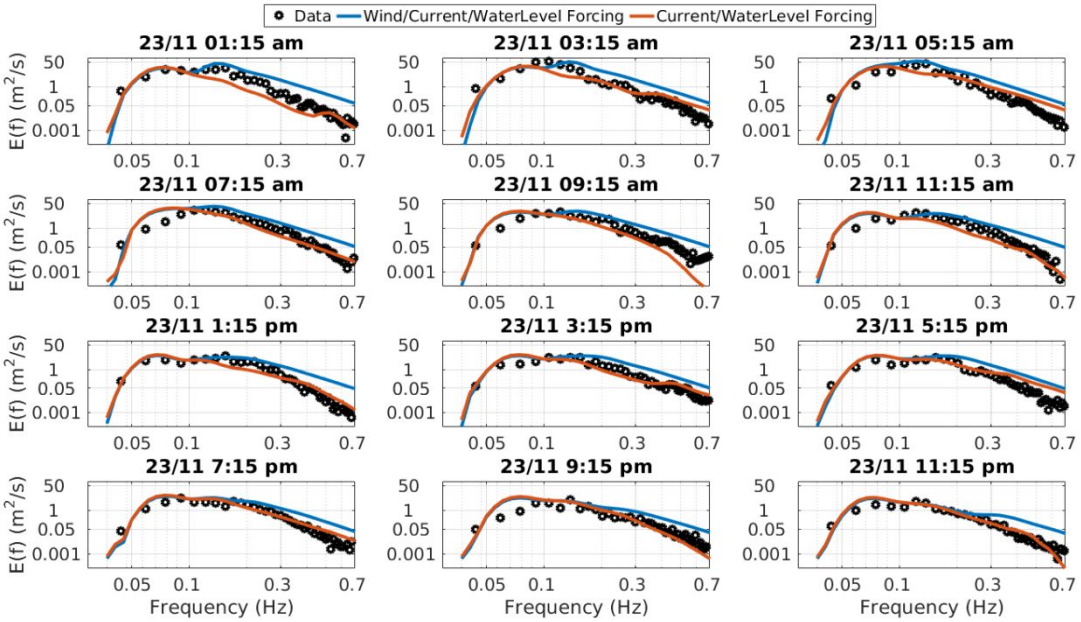

Figure 3: Frequency wave energy spectra at 12 different times of November the 23rd, in 2017 (the times are indicated in the titles). Measurements are represented in black; results of the wave model [19] including the local wind, the water level and the current effects are represented in blue; results of the wave model [19] including the water level and the current effects are represented in orange.

Despite the model uncertainties, the wave model of Bennis et al. [19] highlighted several characteristics of the wave regime in the AR: (i) the significant wave heights are strongly impacted by local wind effects because the wave-to-ocean momentum flux is greatly enhanced by local wind effects ascribed to whitecapping, (ii) the wave directions in the AR are significantly refracted by the tidal current, (iii) tidal currents induce a significant wave energy dissipation by wave breaking when current and waves propagated in opposing directions. Concerning the influence of waves on the current, the model showed that the waves could either reduce or increase the velocity magnitude depending on the angle between the wave propagation and the current direction. For instance, Figure 4 displays the reduction of the current magnitude when the wave and the current directions formed an angle of 60°. This figure also shows that the inclusion of wave effects in the hydrodynamic model reduced the discrepancies between the model predictions and the measurements. It may thus be important to include wave effects in regional models intending to assess the tidal resource of the AR.

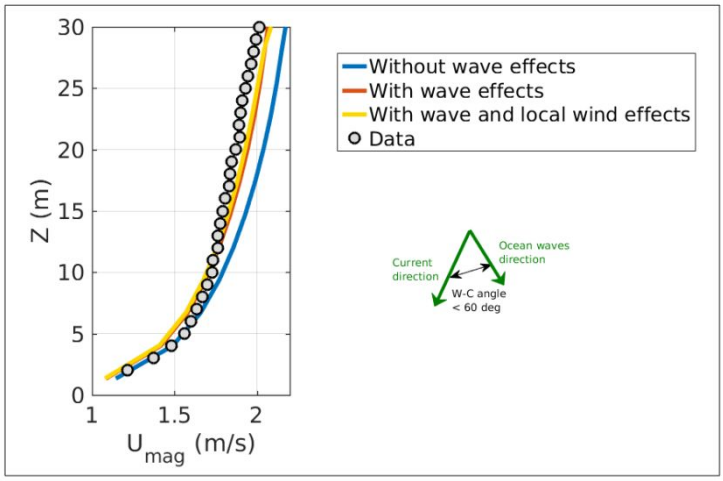

Figure 4: Vertical profiles of tidal current speed (November, the 25th, in 2017, 17:00). The wave conditions were such that H_s (the significant wave height) = 1.6 m, T_p (the peak period) = 6 s and D_p (the peak direction) = 320°/North. Measurements are represented with grey-black circles and numerical results are represented with solid lines (blue line: run without waves, red line: run with wave effects and yellow line: run with wave and local wind effects). This figure has been adapted from [19].

3. Assessment of the Annual Energy Production

The overall objective of tidal resource assessment is to estimate the AEP for a proposed array of turbines. As a reminder, the AEP is the product of the global turbines' output multiplied by the number of hours per year. It is expressed in Wh/year and is calculated as:

$$AEP = n_{hours} \sum_{i=1}^{n} mean(P_i) \qquad (1)$$

where $n_{hours}$is the number of hours per year, n is the number of turbines and P_i is the power output of the i^{th} turbine which is obtained from the tidal flow distribution at the location of the turbine and power curve of the turbine.

We now describe existing studies dedicated to the assessment of the AEP from arrays in AR. This section is limited to studies that consider the energy extraction over large regions of the Race, intended to quantify the AEP potential of the AR. Literature that considers smaller scale arrays is discussed in Section 5.

An upper bound estimate for the energy extraction potential of AR was provided by Coles et al. [1] who considered arrays of turbines spanning the entire width of AR, parameterised through the addition of uniform drag applied over the array area. The array was simulated in a regional scale 2D hydrodynamic model, validated with elevation gauges and ADCP data. The total power extracted from the flow by the array is the product of the free surface elevation drop across the array, and the volume flux through the array. This work quantified the increase in free surface elevation difference across the array, as well as the reduction in volume flux through the array, as a result of added array drag. As the array drag increased from zero, the total power extracted from the flow increased. At the upper bound, any further increase in array drag results in a reduction in volume flux through AR that outweighs any increase in free surface elevation change, resulting in a reduction in power extraction. At this upper bound, the time averaged extracted power, defined as the maximum average power potential, is 5.1 GW. This result was obtained using the M_2 forcing only. It is estimated that this upper bound is achieved with a very high turbine packing density; with lateral and longitudinal spacing between turbines of one and

four turbines diameters, respectively. Adopting more realistic lateral and longitudinal spacing limits of one diameter and ten diameters respectively reduced the average power potential to 3.86 GW. In this case, the average available power, which is defined as the fraction of the average extracted power that is removed by idealized turbines for electricity generation, was estimated to be 1.44 GW, equivalent to an AEP of 12.6 TWh/year. This assumes the turbines have a power coefficient of 0.3, which seems low relative to data from full scale operational turbines in industry that indicate that power coefficients of 0.41 are achievable [51].

Black and Veatch [52] and Owen [53] adopted the kinetic flux method. As the name implies, the kinetic flux is quantified through a cross section of the AR. The level of energy extraction by tidal stream turbines is a proportion of the kinetic flux. In [52], this proportion is termed the Significant Impact Factor (SIF), and is intended to reflect a level of energy extraction that prevents any detrimental impacts to the ambient flow regime. Owen [53] quantified the kinetic energy flux through a 5 km cross-section of AR, with a mean depth of 40 m using velocity data obtained from tidal stream atlases and depths from British Geological Survey maps. This work assumed a SIF of 20%, and provided an estimated AEP of 0.73 TWh/year. In [52], a similar methodology was implemented. Bathymetry data was obtained from hydrographic surveys. This work also assumed a SIF of 20%. The estimated AEP from the flow through a 3.3 km wide cross-section with a mean depth of 33 m was 1.37 TWh/year. In a second phase to this work, velocity data was superseded by data from the Marine Energy Atlas [8]. 1D theoretical channel models were used to estimate suitable SIF values for generic flow regimes based on the assumption that a 10% reduction in mid-range flow velocities or 0.2 m reduction in tidal range ensures ecological systems remain 'relatively unaffected'. This reduced the SIF from 20% to 12%. The cross-sectional width was increased from 3.3 km to 5 km. This increased the average depth of the cross-section from 33 m to 39 m. As a result of these changes the estimated AEP reduced significantly, to 0.37 TWh/year. This work found that flow speed data differed significantly between the tidal stream atlases and the Marine Energy Atlases, an important contributing factor to the reported ±30% uncertainty in AEP estimates.

A third (Phase III) AEP estimate was presented in [54]. In this work, hydrodynamic models were constructed to simulate idealized tidal flow regimes, such as the tidal streaming regime at AR. A tidal streaming regime is defined as the physical response of the tidal system to maintain continuity when a current is forced through a constriction. The model was forced using data from the Marine Energy Atlas. An additional drag term was applied uniformly over a region spanning the width of the AR to simulate the presence of tidal stream turbines. A SIF of 12% was adopted, based upon simulated changes to the ambient flow regime as a result of the added drag. The power potential was estimated using the approach developed by Garrett and Cummins [55], where the energy dissipated by the array is the product of the head loss across the array and the volume flux through the array. This method resulted in an estimated AEP of 2.25 TWh/year. The uncertainty in this Phase III AEP is estimated to be +30%/-45%. Significant contributing factors to this uncertainty are the idealized model geometry, and the discrepancies in the aforementioned tidal flow data used as inputs to the model.

The 'farm method' [6] has been adopted in [56-59]. In this approach, the power generation of individual turbines is estimated from the local hydrodynamic conditions and the power curve of the turbines (which relates the power output of the device to the incoming current velocity magnitude). The power generation of an array is then computed by summing the production of individual turbines. Typically, the flow speeds are obtained from tidal stream atlases. The area considered for energy extraction and installed capacity in these studies is wide ranging, resulting in a wide range of AEP estimates. In [56], the AEP of an array with an installed capacity of 2.4 GW and a spatial coverage of 68 km^2 in depths greater than 20 m is 5.2 TWh/year. In [57], a 1.9 GW capacity array covering an area of 102 km^2 gives an estimated AEP of 6.5 TWh/year. Bahaj and Myers [58] provided an estimate of the energy yield potential from a very large array with a total installed capacity of 3.26 GW. The array consisted of 78 subarrays, where each subarray has 16 dual rotor devices, laid out in two rows of eight devices. Three different rotor diameters (14 m, 20 m, 25 m) and hub heights (14 m, 19 m, 20.5 m) were considered. Each

subarray device rotor diameter and hub height was selected based upon the depth at Lowest Astronomical Tide at the sub-array locations. Six different device ratings were implemented depending on the flow speeds at the location of each sub-array, ranging from 0.75 MW to 9.69 MW. The installed capacity of each sub-array ranged from 12 MW to 155 MW. Typically, larger rotors with lower rated power were used in the deeper West Race where flows are slower, whilst turbines with smaller rotors and higher rated generator power were used in the shallower East Race. Flow speeds were obtained from Admiralty Charts at relatively low spatial and temporal resolution. It was assumed that the wake downstream of the first row of devices within each sub-array leads to a 5% reduction in energy yield of the downstream row. The longitudinal spacing between sub-arrays was maintained at a minimum distance of 500 m, and so it was assumed that there is no sub-array wake impingement on downstream subarrays. The assumed power coefficient of each device was taken as a constant 0.3. The estimated annual energy yield of the whole array using this method is 7.4 TWh/year, which equates to a capacity factor of 26%.

Coles et al. [60] updated the work in [58] by re-estimating the energy yield of the 3.26 GW array using a 2D hydrodynamic model, allowing array scale blockage to be simulated. Results show that the adoption of higher resolution flow data and consideration for array blockage reduces the estimated energy yield of the array by 68%, from 7.4 TWh/year to 2.3 TWh/year. Further discussion on impacts of blockage on the surrounding flow field are provided in Section 4. This result indicates sub-optimal turbine and array design, highlighting the need for turbine specification (rotor diameter and rated power) and turbine placement to be based on the "altered" flow regime after blockage has been characterised. Nevertheless, Coles et al. [60] further demonstrate that through modification of turbine rated power and the implementation of a more representative power coefficient, the array can achieve an energy yield of 3.2 TWh/year whilst also reducing the array installed capacity from 3.26 GW to 2.04 GW. This work also highlights that in light of new, higher resolution bathymetry data, the total swept area of the array could be increased by 32% to improve the power performance further.

The analytical model of Bahaj and Myers [58] has recently been modified by Pinon et al. [61] in order to incorporate the ambient turbulence effects on the energy yield. The modification was based on the experimental data of Mycek et al. [62, 63] who showed that the ambient turbulence affects the velocity recovery in the wakes of turbines and the power coefficient of downstream turbines. Applying their semi-analytical model to the AR, they showed that turbulence greatly influences the AEP. Another AEP assessment was presented by Myers and Bahaj [59] who considered a different configuration of 75 sub-arrays with a total installed capacity of 1.5 GW in the AR. Each sub-array consisted of 20 single rotor devices, set out in two rows of ten turbines. The blade element momentum package Bladed was used to characterise the power coefficient of pitch controlled, fixed speed turbines. This resulted in a power coefficient that exceeded 0.4 over the majority of the below rated speeds. The level of wake impingement on downstream rows of turbines was estimated using momentum theory. The estimated annual energy yield of the 1.5 GW array was 1.3 TWh/year, equivalent to a capacity factor of 10%. Finally, Campbell et al. [11] also evaluated the AEP of different tidal energy sites located along the coast of France using the 'farm method'. In the AR, an area of 171 km^2 was selected, wherein the mean current speed exceeds 1.5 m/s and the depths range between 10 and 60 m. Different turbine power coefficients and turbine densities were considered. In their 'medium' scenario (which specified a power coefficient of 0.35 and longitudinal and lateral spacings of 12*D* and 4*D* respectively, with *D* the turbine diameter), the turbines produced 9.91 MW per square kilometre. Multiplying this mean power output by the surface, they obtained a mean turbine output of 1.7 GW, equivalent to 14.9 TWh/year. It is however important to note that their estimation relied on the cube of the mean velocity (rather than on the mean of the cubed velocity, as recommended in the standard methodology, e.g. [7]), which may strongly affect their estimates (to give an order of magnitude, we used a time-series of tidal currents extracted in the AR (from [22]). This

application showed that, at the selected location, the cube of the mean velocity is 43% smaller than the mean of cubed velocity). Table 2 gives an overview of the aforementioned AEP assessment.

References	Year	Method	Hydrodynamic data	AEP
Energy Technology Support Unit (ETSU) [56]	1993	Farm method, based on an array covering 65 km^2	Tidal stream atlases	5.20 TWh/year
European Commission [57]	1996	Farm method, based on array covering 102 km^2	Tidal stream atlases	6.50 TWh/year
Bahaj and Myers [58]	2004	Farm method, based on a 3.26 GW array covering Alderney Race	Tidal stream atlases (Admiralty Charts)	7.40 TWh/year
Black and Veatch/ Carbon Trust, Phase 1 [52]	2005	Kinetic flux method based on a 3.3 km cross section of AR	Tidal stream atlas (British Geological Survey)	1.37 TWh/year
Myers and Bahaj [59]	2005	Farm method based on a 1.5 GW array covering Alderney Race	Tidal stream atlases (Admiralty Charts)	1.35 TWh/year
Black and Veatch/ Carbon Trust, Phase 2 [52]	2005	Kinetic flux method based on a 5 km cross section of AR	Tidal stream atlas (Marine Energy Atlas)	0.37 TWh/year
Owen et al. [53]	2005	Kinetic flux method based on a 5 km cross section of AR	Tidal stream atlas (British Geological Survey)	0.73 TWh/year
Black and Veatch/ Carbon Trust, Phase 3 [54]	2011	Method of Garrett and Cummins [25], based on an array covering 61 km^2	Tidal stream atlas (Marine Energy Atlas)	2.25 TWh/year
Coles et al. [1]	2017	Upper boundestimate based on fence array spanning width of AR with 'practical' turbine density	Telemac2D (M_2)	12.60 TWh
Campbell et al. [11]	2017	Farm method based on an array covering 171 km^2	MARS2D	14.90 TWh/year
Coles et al. [60]	2020	Continuous drag method, based on the same array layout in [58], but with an array capacity of 2 GW	Telemac2D (10 constituents)	3.18 TWh/year

Table 2: Summary of the method and estimated AEP of studies in AR.

4. Impacts of tidal turbines on physical conditions

Numerous investigations have shown that the exploitation of the tidal stream resource could significantly impact the sediment transport and hydrodynamics in the regions surrounding tidal energy sites [60, 64]. Examples of impact assessment studies can be found in the Pentland Firth [65, 66], in the Bay of Fundy, Gulf of Maine [67], the Fromveur Strait, France [68], and the AR [17, 22, 60]. In these regional scale studies, the effect of arrays is generally represented in numerical models through the inclusion of an additional momentum sink term in the momentum equations (either 2D or 3D) which

exerts, on the flow, a force that is equivalent to the thrust (and also the drag in several studies) of the turbines. This approach is known as the distributed drag or continuous drag method. As the sink term, denoted $\vec{S}$ in (2), has a comparable formulation to the bed friction term (it depends on the squared current velocity), this methodology for representing the turbines is often referred as 'bed friction' or 'enhanced drag'.

$$\vec{S} = -n\frac{1}{2}\rho C_T A\|\vec{U}\|\vec{U} \qquad (2)$$

where n is the number of turbines, ρ is the water density, A is the area swept by the blades of a turbine, C_T is the thrust coefficient, $\vec{U}$ is current velocity vector, and $\|\vec{U}\|$ is the current magnitude.

We now present several investigations, dedicated specifically to the AR, where numerical models using the enhanced drag approach have been applied to understand the potential impact of arrays. We start by considering the effects on the hydrodynamics. Thiébot et al. [22] investigated the effect of two hypothetical 290 MW array sited in the vicinity of the Cap de la Hague (French part of the AR) with Telemac2D. Their hydrodynamic model, applied at a resolution of 150 m in the AR, was embedded within a large-scale model covering the NW European shelf [13]. The validation of the tidal current and free surface elevation relied on the measurement database of [13], including four ADCP time-series and four month-long measurements of elevations at three tide gauge stations. The simulations with turbines showed that, in line with comparable studies at other sites, the monthly mean current velocity magnitude is reduced by 15% (in comparison to the baseline velocity magnitude) in the zone occupied by the turbine array, and that a slight increase of current magnitude is observed along the boundary of the tidal farm. The effects of the turbines persisted several kilometres from the extraction zone (Figure 5). Using a comparable approach but considering larger tidal farms (extending over the entire width of the Race), Coles et al. [1] showed that extracting tidal energy in the AR induced far-field perturbations to the current and modified the resource at other potential tidal energy sites in the Channel Islands: Casquets, located on the western side of the Island of Alderney, and Big Roussel, sited 40 km south of the AR. They also showed that the flow diversion caused by extracting tidal energy in the AR is beneficial to the Casquets site where it increased by 68% due to power extraction. This result suggested that developers should strategically work together to optimize the energy extraction in this region, which has been confirmed by investigations relying on array-design optimisation models (which is discussed in section 5).

As discussed in Section 3, Coles et al. [60] characterised the change in the hydrodynamics caused by a large array in AR. The array considered in this work is the same array that was first considered by Bahaj and Myers [58]. Results show that array blockage reduced flow speeds within the array by up to 2.5 m/s during spring tides, whilst also increasing flow speeds in the regions around the array by up to 1 m/s. The array blockage reduced the mean volume flux through AR by 8%. Based on the findings in this work, it was concluded that further array design work is required to mitigate any detrimental environmental impacts whilst also improving array power performance.

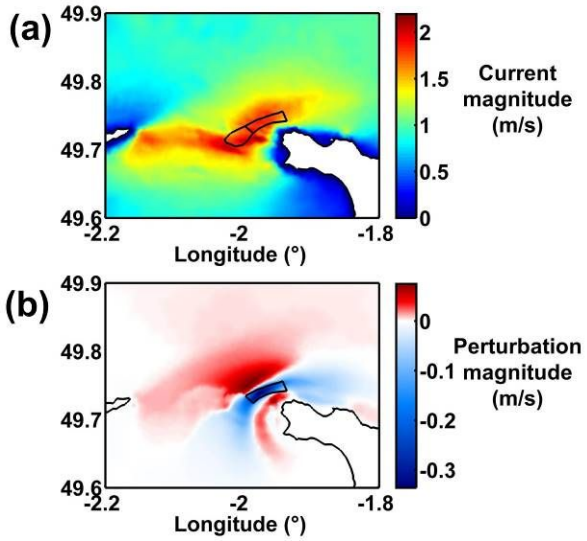

Figure 5: Impact of a 290 MW array on the mean current velocity magnitude: (a) baseline; (b) changes induced by a tidal farm. The results are averaged over a 1-month-long simulation. Reprinted from [22] Thiébot et al. (2015) Numerical modelling of the effect of tidal stream turbines on the hydrodynamics and the sediment transport – Application to the Alderney Race (Raz Blanchard), France. Renewable Energy, Vol. 75, pp. 356-365. Copyright 2020, with permission from Elsevier.

As tidal energy extraction modifies the flow field, it also perturbates sediment transport processes. Changes in sediment transport are more pronounced than changes to the flow field because sediment transport is a function of a higher power of the velocity magnitude. Investigations were thus conducted to assess the impact of turbines deployed in the AR on the sediment dynamics. Neill et al. [17] investigated the effect of an array of 200 x 1.5 MW tidal turbines on the dynamics of the Alderney South Banks located in the vicinity of Alderney. Their investigations relied on a 3D model POLCOMS configuration with a horizontal resolution of 150 m and 20 terrain following (sigma) levels. Their model, forced by the M_2 and S_2 constituents, was validated with elevations measured by three tidal gauges and current data taken from Admiralty Charts. The morphodynamic model was based on the total (bedload and suspended) sediment transport formula of [69-71], and the Exner equation was used to compute the evolution of the sea bed. From maps of residual sediment transport (Figure 6a), they first highlighted the presence of a residual eddy coinciding with the location of the South Banks. Then, they investigated the influence of two possible arrays of 200 turbines deployed in this zone and showed that the tidal energy extraction strongly reduced the magnitude of the sediment transport (Figure 6b), which caused a considerable morphodynamic change of the sand banks (Figure 6c). Those investigations on the South Banks were further complemented by Blunden et al. [72] with additional data (i.e. high resolution bathymetry and ADCP data collected in the immediate velocity of the sandbank), which enabled a refined model validation in terms of velocity predictions and sediment transport residual (inferred from sand-wave migrations). Considering seventeen possible locations for a 300 MW array, Blunden et al. [72] showed that the patterns of erosion were sensitive to the distance between the array and that the modification of the residual sediment transport were strongly asymmetrical which led to complex patterns of erosion/deposition and a possible shift of the banks. Thiébot et al. [22] also investigated the effects of tidal energy extraction in the AR (considering two hypothetical 290 MW array located northwest the Cap de la Hague). Their simulations with turbines showed that tidal energy extraction might cause significant changes in the distribution of surficial sediment types and in the bedload transport because the turbines significantly modified the spatial distribution of the bottom shear stress. Modifications to the sediment regime were strongly asymmetrical and dependant on the location retained for deploying the array. This is a finding that is consistent with Neill et al. [17] and Blunden et al.

[72]. In addition, Thiébot et al. [22] also investigated the effect of the turbines on the suspended sediment transport. Comparisons of the area of deposition of sediment predicted by the model with and without turbines were made. The baseline simulations showed that the greatest part of the suspended sediments that transited through the AR naturally deposited in the eastern part of the English Channel. Extracting tidal energy could significantly alter this mass balance between the two sides of the English Channel. Furthermore, the perturbation was found to be dependent on the location of the array. Although the aforementioned sediment transport models permitted to investigate the potential impacts of tidal turbines in the AR, it is worth reminding that neither the sediment transport, nor the impact of tidal energy extraction on sediment dynamics, has been validated (except the sand-wave migrations reported in [72]).

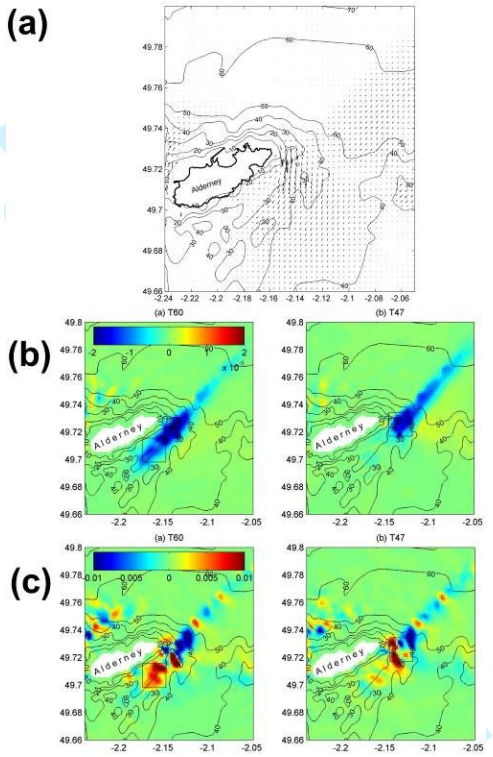

Figure 6: (a) Residual sediment transport. (b) Change in the volumetric sediment transport rate (in m^2s^{-1}) due to energy extraction, averaged over a spring-neap cycle. (c) Change in bed level (in m) due to energy extraction, averaged over a spring-neap cycle. The boxes show the limits of the array. Reprinted from [17] Neill et al. (2012) Impact of tidal energy converter (TEC) arrays on the dynamics of headland sand banks. Renewable energy, Vol 37, n°1, pp. 387-397. Copyright 2020, with permission from Elsevier.

5. Array design testing and optimisation

According to Vennell et al. [73], maximising the tidal power extraction requires consideration of both the 'macro-' and the 'micro-design' of tidal energy farms. Whereas the macro-design determines the density of turbines that maximises the farm efficiency according to the possible flow diversion and the reduction of the enhanced hydraulic resistance, the micro-design can boost the output by adjusting individual turbines' positions, taking into account wake effects. Both of these design aspects have been considered in the AR. In this section, we first present the macro-design studies and then present the micro-design investigations.

The AR has attracted interest for tidal energy projects in both the French and the Alderney territorial waters (in the eastern and the western part of the Race, respectively). As the development of large-scale projects is envisaged on both sides of the Race, significant modifications of the current structure are expected, especially a flow redirection around arrays and a reduction of the ambient velocity in the array wake. Thus, if several tidal energy projects emerge in the Race, array-array interactions, with either complementary or detrimental effects, are expected. It is therefore important to test and compare different scenarios of development to optimise the design of large-scale arrays. This issue has been investigated with models that optimize the location and the density of turbines [74, 75]. These investigations rely on the coupling between (i) 2D nonlinear shallow water solvers in which the turbines are represented with an enhanced drag term (as in section 4) and (ii) an algorithm optimising the spatial distribution of the turbines' density. The objective is to establish the optimal spatial distribution of turbines (limited by a maximum array density) for a user-defined performance indicator, which may be to maximise electricity production or minimise Levelized Cost of Energy (LCoE), for example.

Coles et al. [74] and Goss et al. [75] pursued comparable objectives but used different optimisation models. The investigations of Coles et al. [74] used the software package OpenTidalFarm [76] in which the optimisation was performed *via* a gradient-based method. In this initial study, the hydrodynamic conditions were simplified significantly by considering steady state flows (representative of either the peak flood or peak ebb tide) and uniform bathymetry over the domain. The array density was optimised to maximise the profit of the array, which was the difference between the revenue (which depended on the amount of electricity sold) and the capital cost (which was assumed to scale linearly with the number of turbines). The results showed that it was advantageous to deploy the turbines using one or two fence-like structures oriented perpendicular to the flow. When the array did not extend over the entire Race (turbines deployed in either the French or the Alderney territorial waters), the optimised layout has a 'U' shape. In this case, the 'strips' of turbines located parallel to the flow 'contained' the flow, preventing it from redirecting around the array. Goss et al. [75] complemented the investigations of Coles et al. [74] with the Thetis model (an extension of OpenTidalFarm), which integrated the same adjoint approach to find the optimal spatial distribution of turbines. Although the hydrodynamics was more realistic than in [74], the hydrodynamic conditions were still highly idealised. Indeed, as the iterative process of optimisation required many hydrodynamic simulations (until the model found the optimized spatial distribution of turbines), the hydrodynamic simulation was run for only 2 days (at each iteration) and was driven by only the M_2 tidal constituent. Another difference with [74] was the choice of the objective function. Goss et al. [75] opted for a function that only depended on the power generated by the array. As this function was independent of the costs of the turbines, the model could deploy turbines (even if they were costly) until the flow rate and the generated power started to decrease. Despite the differences in those two optimisation methods (realism of the tide, objective functions), it is interesting to notice that the findings of Goss et al. [75] and Coles et al. [74] are in line with one another. Both investigations showed that the most efficient layout consisted in spacing out the turbines across the northern part of the Race and in placing a second fence crossing the southern part of the Race. This is highlighted in Figure 7, which displays the control parameter to be optimised, noted c_t, which is equal to $0.5C_TAd$, where $C_T$is the thrust coefficient (C_T= 0.8), A is the area swept by the blades and d is the spatial density of the turbines. Goss et al. [75] also found that, when the array partially occupied the Race, adding a strip of turbines parallel to the flow 'contained' the flow, avoiding redirection of the flow around the fence of turbines (Figure 7b). Finally, they showed that the overall regional development strategy (turbines deployed in either French or Alderney territorial waters, turbines deployed in both territorial waters with or without cooperation) had a significant impact on the shape of the layout (Figures 7a and 7b) and on the total power that could be harnessed from the AR.

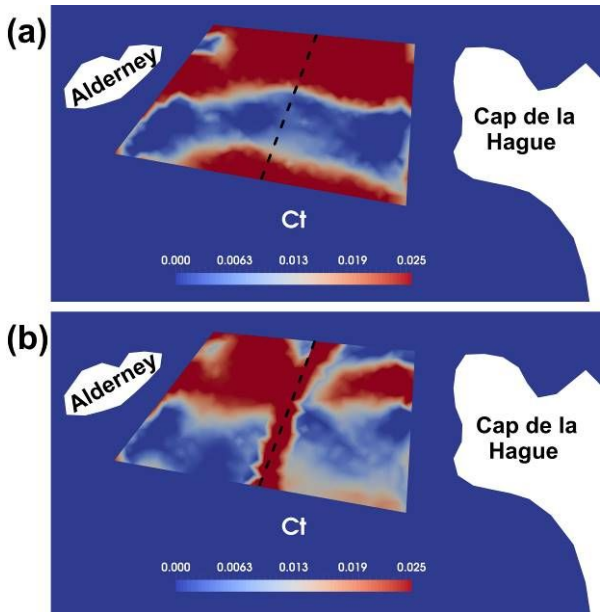

Figure 7: Optimised spatial distribution of tidal turbines. (a) French and Alderney cooperate to maximize the total power. (b) The two regions develop with no knowledge of the other array in the design stage. Adapted from the Figure 5a and 5b of Goss et al. (2018) [75] Competition effects between nearby tidal turbine arrays - optimal design for Alderney Race. *Advances in Renewable Energies Offshore*. Editor: C. Guedes Soares. Taylor and Francis. pp. 255 - 264.

Within a tidal array, energy extraction causes changes to the ambient flow regime. This is seen through reduction in the velocity in the wakes of the turbines and a fluid acceleration in the bypass flow surrounding the turbines/wakes – sometimes termed local blockage. Those changes impact the individual and global output of the turbines, and it is thus important to find the optimal arrangement of turbines that maximises the AEP of the tidal farm. Complementary to the studies mentioned above that focused on the global effects of large arrays on the dynamics of the entire Race, Lo Brutto et al. [77] proposed a method to optimize the micro-design of smaller tidal farms, using the AR as a case study. This work optimised the turbine arrangement by focusing on the effects of the wake interactions on the AEP. Following earlier works on the design of wind farms, they used particle swarm optimisation to find, *via* an iterative procedure, the turbine arrangement that minimized the ratio between the cost of the turbines and the output of the array. In their algorithm, the candidate turbine arrangements were represented with a (n x n) grid where each node represented a possible location for a turbine (the node value was 1 if the algorithm chose to deploy a turbine and 0 otherwise). As the number of turbines was free, there were 2^n possible turbine arrangements. The changes of the flow field within the tidal farm (for a given arrangement) were computed with a simplified momentum equation (balance of momentum between the upstream and the downstream sides of the turbines) which was derived from the approach proposed by Jensen [78, 79] for the design of wind farms [80]. Different ambient hydrodynamic conditions were considered to force the wake-field model, including conditions representative of the AR provided by the 2D model of Thiébot et al. [22]. The results of the optimisation model showed that when the ebb and flood currents are well-aligned, the layout that maximised AEP was to position turbines in fences oriented perpendicular to the flow (as shown in Figure 8a). The optimal longitudinal distance between consecutive fences was highly dependent on the ambient turbulence. Lo Brutto et al. [77] also highlighted that at the locations of the AR where there was a current misalignment (between ebb and flood phases of the tidal cycle), it was preferable to distribute the turbines as evenly as possible over the tidal farm (as shown in figure 8b).

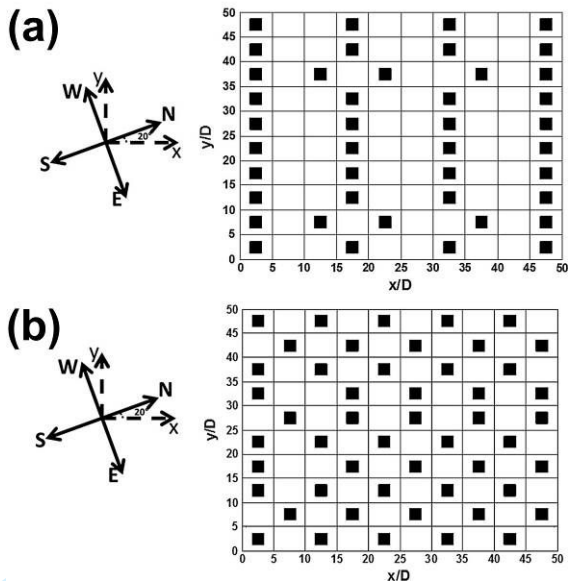

Figure 8: Influence of the current misalignment on the optimal tidal array layout. Optimal layout obtained with the hydrodynamic data of the Alderney with bidirectional flows (a), and with misalignment between ebb and flood phases of the tidal cycle (b). The predominant current direction is parallel to the x-axis. Reprinted from [77] Lo Brutto et al. (2016) A semi-analytic method to optimize tidal farm layouts – Application to the Alderney Race (Raz Blanchard), France. Applied Energy. Volume 183, Pages 1168-1180. Copyright 2020, with permission from Elsevier.

Hundreds of iterations are required before reaching convergence when optimising the micro-design of tidal farms with a model such as that developed by Lo Brutto et al. [77]. As the computation of the wake-field (and the assessment of the associated turbines' output) is repeated many times, it should be achieved in a reasonable period of time to avoid prohibitive computational cost. The hydrodynamic model used to compute the flow interaction between turbines is thus highly simplified. Indeed, the Jensen' model only considers the reduction of the flow velocity in the turbines' wakes and relies on an empirical wake expansion model [81]. Numerous processes are therefore neglected such as the 3D effects or the flow acceleration around the turbines due to blockage effects. Furthermore, mixing processes are highly simplified as the turbulence is assumed to be uniform within the array (i.e. the effect of the wake-added turbulence is not considered). The results of optimisation models should therefore be complemented with array testing, relying on more reliable hydrodynamic models. Using the AR as a case study, several wake field studies [20, 82, 83] were thus performed to compare a limited number of turbine arrangements (fixed *a priori*) and to analyse the influence of the hydrodynamic characteristics, the type of arrangement (e.g. staggered or aligned), and the distance between turbines on the array output.

The interactions between horizontal-axis turbines deployed in array was investigated by Nguyen et al. [82] and Thiébot et al. [20] with 3D RANS models in which the turbines were represented by Actuator Disk theory, hereafter AD. This technique applies a momentum sink across the swept area of the turbine rotors that is equivalent to the turbine thrust. AD models neglect important processes such as swirl generated by the rotation of the turbine blades, and the unsteady flow characteristics or the tip vortices shed by the blades. However, those processes may dissipate rapidly behind the turbine and numerous AD models validated against experimental data on scaled turbines have demonstrated that AD can give reliable estimates of the flow in the mid- to far-wakes (at distance from the turbines greater than five turbine diameters) provided that the unresolved processes are properly simulated by the turbulence model [28, 84]. Although the turbine representation (based on the AD concept) is comparable between [82] and [20], those two wake-field studies differed as shown in Table 3, which summarises the main

characteristics of these investigations. Nguyen et al. [82] showed that the staggered layout was more efficient than the aligned layout when the current was rectilinear and that, when there was variation in the current direction, there was less benefit in using a staggered layout (in comparison to the aligned layout). In line with this finding, Thiébot et al. [20] also demonstrated that the staggered layout gave a greater AEP than the aligned layout, especially when the lateral distance exceeded 5D. Notably, Thiébot et al. [20] also highlighted the effect of the wake-added turbulence on the flow recovery in the wake of the turbine, which has strong implications on the choice of the longitudinal distance between two consecutive rows of turbines.

Reference	[82]	[20]
3D Solver	ANSYS Fluent	Telemac3D
Model settings	Steady RANS equations Finite Volume Turbulence model : k-ε Hexahedral elements	Unsteady RANS equations Finite Element Turbulence model : k-ε Prismatic elements (triangular cell extruded over the vertical using σ-layers)
Domain size	Restricted to the area occupied by the array (680 m x 804 m)	English Channel with refinement in the area occupied by the array
Tested layout	9 aligned turbines (3 rows), 10 staggered turbines (3 rows)	Isolated turbine, 4 staggered layouts, 4 aligned layouts (with different spacings between devices)
Hydrodynamic conditions	Current data representative of different times of a mean tide. Rectilinear flow and misalignment between ebb and flood flow.	1 spring tide. Realistic tidal conditions (3D model forced validated with ADCP data).

Table 3: Main characteristics of the wake field studies using the AR as a case study.

To gain more insight into the local processes affecting turbine loading and performance, more advanced computational techniques should be used, such as models applying Boundary Element Momentum Theory or blade-resolved models. The latter method was utilised by Zanforlin [83], who investigated the flow interactions between three closely spaced vertical-axis turbines (with a diameter of 1 m) deployed in the AR. They considered two different layouts: (i) a single fence (perpendicular to the flow), and (ii) a triangular layout. The 2D simulations were performed with ANSYS Fluent. The turbulence was modelled with the k-ω SST (SST stands for Shear Stress Transport). To compare the performances of the two layouts on a realistic scenario of tidal energy extraction, Zanforlin [83] tabulated the power obtained for different ambient current orientation and magnitude, and used those results to compute the energy yield over a six month period in the AR. The hydrodynamic data was obtained from British Admiralty Charts. They concluded that the side-by-side layout was more advantageous than the triangular layout because it enabled a two and a half greater gain than the triangular layout (in comparison to an isolated turbine). They also concluded that the rectilinearity of the current in the AR maximized the efficiency of the side-by-side array.

6. Conclusion and perspectives

Harvesting the tidal current resource of the Alderney Race could provide a vast amount of low-carbon electricity (on the order of GWs). Indeed, the surface area over which the tidal current magnitude is sufficiently high to deploy turbines is very large (dozens of km^2), which enables the deployment of a large number of devices. This site has therefore been considered as a case study for numerous investigations, most of which rely on numerical modelling. These modelling studies covered different aspects of tidal energy in the AR such as the hydrodynamic characterisation, the assessment of the AEP, the impact of tidal arrays on the environment, and the optimisation of array design.

Studies that have characterised the hydrodynamics in AR have used a range of temporal and spatial scales. Large-scale models encompassing different sites of the NW European shelf showed that, in comparison to the other sites, both the variability between spring and neap flow and the current asymmetry between peak ebb and flood are relatively low in the AR, which is desirable for integration of the electricity into the grid. Most field data acquired in the AR are protected (especially the ADCP data). Therefore, the dataset used to calibrate and validate the models are generally sparse, restricted to particular regions of the Race and not always processed according to the latest standards [7]. This lack of spatial coverage leads to uncertainties when models are applied in a region of the Race where data are not available. Refined models of the AR were generally validated with different model performance indicators. Indeed, whereas several works were based on the characteristics of the tidal constituents (e.g. amplitude/phase, and tidal ellipses), other studies relied on comparisons between predicted and measured time-series of current velocity or water level (and the resulting RMS errors). It is thus difficult to compare the models and to draw general conclusion as regards the appropriate model settings (e.g. number of tidal constituents and source of boundary data, accuracy and resolution of the bathymetry data, necessity to include the wave/meteorological forcing, mesh resolution and simplification of the seabed geometry, 2D vs 3D, choice of bed friction law, etc…). Despite a lack of common methodology, existing studies showed that the more advanced models were able to capture the main characteristics of the tide with RMS errors of order 0.25 m/s, phase-lags of order 5°, and amplitude errors less than 10%. Despite good model performances in terms of velocity magnitude, uncertainties in power density are expected to be significant as they depend on the cube of the computed current velocity magnitude. These uncertainties in the estimates of the cubed velocities could have a significant influence on the AEP assessment or the design of arrays. In future work, it would thus be useful to estimate model discrepancies in the cubed velocities. Other actions could also be taken to reduce uncertainties in resource assessments of the AR: following technical specification [7] with the objective of harmonizing the modelling strategies and the presentation of the results, organizing a modelling benchmark to identify best practices, encouraging the sharing of data, and making extensive hydrodynamic dataset (with a wider spatial coverage and with a large range of tidal/meteorological conditions) available to modellers. Of note, two projects (HYD2M and THYMOTE) recently collected a large amount of field data in the French territorial waters including waves and surface currents monitored with HF oceanographic radar [85, 86], turbulence [36-38], waves and currents measured by towed and bottom-mounted ADCPs [87], wind measurements, etc. This recent dataset, presented in several articles of this special issue, is expected to help further improve the numerical models of the AR.

In addition to refined modelling of the tidal dynamics, turbine developers require reliable estimates of the loading conditions encompassing the effects of waves and turbulence. Developments are likely to arise in this field. Indeed, the Large Eddy Simulations of Mercier et al. [34] and Bourgoin et al. [31] agreed well with the turbulence measurements acquired in the AR. Their work using LES also paved the way to a better understanding of the dynamics of the largest eddies that may impact the tidal turbines deployed in the AR. Using the LANS-α and the Leray-α turbulence models, Adong and Bennis [21] also highlighted the interest in going beyond the RANS approach to improve turbulence modelling in the AR. Wave modelling in the AR is sparse at present. The reference sea state dataset has been built by Boudière et al. [44] who forced a spectral model (WaveWatch-III) by a 2D hydrodynamic model. This dataset can

be used to characterise, as a first approach, the wave regime in the AR. However, the model has not been validated with data acquired in the AR (where the waves are expected to have a particular dynamics). Complementing this approach, Bennis et al. [19] have recently shown that the use of more advanced wave model methodologies (3D fully-coupled wave-current model) reduced uncertainties in the estimation of sea states. They also demonstrated that the inclusion of waves and winds in their model increased the model performance when predicting current velocity (and the associated tidal energy resource).

The estimated maximum average power potential from M_2 forcing in the AR is 5.1 GW, 35% greater than the well-known Pentland Firth in Scotland [1]. Whilst this supports the theory that the AR has the potential to contribute significantly to future green energy supply, the level of energy that could practically be harnessed remains less clear. Results from the literature reviewed in this paper show that the estimated AEP potential from large arrays in the AR range from 0.37 TWh/year [52] to 14.9 TWh/year [11]. Reasons for this range in AEP estimates include differences in spatial and temporal resolution of velocity and bathymetry data. Such uncertainties could easily be reduced by using more detailed hydrodynamic data (such as those presented in this review). Sources of difference between the assessments are also as a result of differences in array design (i.e. spatial coverage of arrays, installed capacity and turbine siting) and (c) turbine design (i.e. rated power, rotor diameter, hub height and power coefficient) and modelling approach. Indeed, whereas several assessments consider the possibility to deploy turbines over the entire Race (without technical and environmental constraints), others focus on a small cross-section of the Race. Finally, (d) modelling approaches also differ from one study to another, which prevents from comparing directly the different AEP estimates.

Global array optimisation studies [74, 75] have helped improve understanding of how array design within the AR can maximise AEP. The adjoint-based optimisation approach has helped optimal array design to converge, whilst also highlighting the need for collaboration between developers in Alderney and French Territorial Waters. A limitation to these models is that they remain idealised to some extent, and so work in developing the models to reduce uncertainty is important.

Complementing the models mentioned above (adapted to the design of large arrays), models dedicated to the micro-design of tidal farms may also help to optimise AEP by adjusting the arrangement of turbines within an array. Different types of micro-design models have been applied to the AR. With a semi-empirical wake model and a particle swarm optimisation model, Lo Brutto et al. [77] adjusted the density and positions of turbines in order to maximise the profit of a potential array in the AR. Using a more reliable approach to simulate the flow within the array, Nguyen et al. [82] and Thiébot et al. [20] compared different turbine arrangements chosen *a priori*. Their wake-field studies, relying on a 3D solver in which the turbines are represented as Actuator Disks, confirmed the advantage of staggering the turbines, in comparison to an aligned layout. They also highlighted the influence of the rectilinearity of the tidal currents on the performance of the array. Those models intending to optimise the layouts give general recommendations in order to optimise the energy extraction or the cost of energy. In the aforementioned studies, they have been applied in idealised/simplified configurations. It is however important to keep in mind that other constraints may affect the choice of turbine layouts in real-world applications: constraints on electrical topology (length/cost of the electric cables, distance to the shore…) or the maintenance (minimum clearance between devices), regulatory/environmental constraints...

Finally, uncertainty in hydrodynamic characterisation or AEP potential of the AR also stems from the level of environmental impacts of large-scale energy extraction. This has been investigated with respect to the Alderney sand banks, for example. It is important that future AEP assessments consider energy extraction and resulting changes to the flow regime in order to prevent any detrimental impacts.

Additional Information

Data Accessibility
This article has no data.

Funding Statement
Jérôme Thiébot and Sylvain Guillou acknowledge the Interreg VA France (Channel) England Programme which funds the TIGER project and the French State support programme managed by the National Research Agency under the Investments for the Future program which funds the THYMOTE project (reference ANR-10-IEED-0006-11). Daniel Coles acknowledges the support of the International Centre for Infrastructure Futures (ICIF) (EP/K012347/1). The work of Anne-Claire was performed in the framework of the HYD2M project (French State support managed by the National Research Agency under the Investments for the Future program bearing the reference ANR-10-IEED-0006-07). The contribution of Nicolas Guillou was performed as part of the research program DIADEME ("Design et InterActions des Dispositifs d'extraction d'Energie Marine avec l'Environnement") of the Laboratory of Coastal Engineering and Environment (Cerema, http://www.cerema.fr). Simon Neill acknowledges the support of SEEC (Smart Efficient Energy Centre) at Bangor University, part-funded by the European Regional Development Fund (ERDF), administered by the Welsh Government.

Competing Interests
We have no competing interests.

Authors' Contributions and acknowledgments
As this article is a review, the authors' contribution consisted in concepting and designing the article and in revising it critically. The authors' contributions were shared in the following way: the 'hydrodynamic characterisation and assessment of the AEP' section was mainly written by DC, JT, SN, NG, MP and SG. The main contributors to the 'Ambient turbulence and wave climates' section are ACB, JT and SG. The 'Impacts of the tidal turbines on the physical conditions' section has been principally written by JT, SN, and NG. The 'Array design testing and optimisation' section has been written mainly by DC, MP, JT and SN. All authors approved the manuscript.
The authors warmly thank Zoe Goss and Peter Robins who shared their figures.

References

1. Coles D.S., L. S. Blunden, A. S. Bahaj. 2017. Assessment of the energy extraction potential at tidal sites around the Channel Islands. *Energy*, **Vol. 124**, pp. 171-186.
2. European Environment Agency. 2014. Energy support measures and their impact on innovation in the renewable energy sector in Europe. EEA Technical report. Additional File 'France'. N° 21/2014. doi:10.2800/25755. 70 p.
3. ADEME. 2018. Etude stratégique de la filière hydrolien marin. 38 pages (in French).
4. Simec Atlantis. 2018. accessed 20 January 2020, https://simecatlantis.com/2018/11/21/french-tidal-power-one-step-closer-to-commercialisation-as-simec-atlantis-spearheads-normandie-hydrolienne-jv/.
5. Hydroquest. 2019. accessed 25 May 2020, https://cmn-group.com/hydroquest-ocean-6-mois-de-fonctionnement-continu/
6. Legrand C. 2009. Assessment of tidal energy resource. Published by BSI, UK. ISBN 978-0-580-65642-2.

7. IEC-TS 62600-201. 2015. Marine Energy Wave, Tidal and Other Water Current Converters Part 201: Tidal Energy Resource Assessment and Characterisation.
8. DTI, Marine Energy Atlas. 2007. http://www.renewables-atlas.info/. [Date Accessed: 14/12/2019].
9. SHOM, https://data.shom.fr/. [Date Accessed: 18/05/2020].
10. Robins P.E., S.P. Neill, M.J. Lewis, S.L. Ward. 2015. Characterising the spatial and temporal variability of the tidal-stream energy resource over the northwest European shelf seas. *Applied Energy*, **Vol. 147**, pp. 510-522.
11. Campbell R., A. Martinez, C. Letetrel, A. Rio. 2017. Methodology for estimating the French tidal current energy resource. *International Journal of Marine Energy*, **Vol. 19**, pp. 256-271.
12. Guillou N., S.P. Neill, P.E. Robins. 2018. Characterising the tidal stream power resource around France using a high-resolution harmonic database. *Renewable Energy*, **Vol. 123**, pp. 706-718.
13. Bailly du Bois P., F. Dumas, L. Solier, C. Voiseux. 2012. In-situ database toolbox for short-term dispersion model validation in macro-tidal seas, application for 2D-model. *Continental Shelf Research*, **Vol. 36**, pp 63-82.
14. Thiébaut M., A. Sentchev, P. Bailly du Bois. 2019. Merging velocity measurements and modeling to improve understanding of tidal stream resource in Alderney Race. *Energy*, **Vol. 178**, pp. 460-470.
15. Pal R.K., K. Lakshmanan, S. Narasimalu. 2018. Tidal Resource Modeling: Alderney Race. *Proc. of the 2018 Asian Conference on Energy, Power and Transportation Electrification*, 8p.
16. Blunden L.S., A.S. Bahaj. 2005. A high resolution model of the English Channel for tidal stream resource assessment. *6th European Wave and Tidal Energy Conference*. Glasgow, UK. pp. 51-58.
17. Neill S.P., J.R. Jordan, S.J. Couch. 2012. Impact of tidal energy converter (TEC) arrays on the dynamics of headland sand banks. *Renewable Energy*, **Vol. 37(1)**, pp. 387-397.
18. Neill S.P., A.J. Elliott, M.R. Hashemi. 2008. A model of inter-annual variability in beach levels. *Cont Shelf Res*, **Vol. 28**, pp. 1769-1781
19. Bennis A.-C., L. Furgerot, P. Bailly du Bois, F. Dumas, T. Odaka, C. Lathuilère, J.-F. Filipot. 2020. Numerical modelling of three-dimensional interactions in a complex environment: application to Alderney Race. *Applied Ocean Research*, **Vol. 95**, Article 102021, 15 p.
20. Thiébot J., N. Guillou, S. Guillou, A. Good, M. Lewis. 2020. Wake field study of tidal turbines under realistic flow conditions. *Renewable Energy*. https://doi.org/10.1016/j.renene.2019.11.129.
21. Adong F. and A.-C. Bennis. 2019. Turbulence models for coastal simulation: application to Alderney Race. *Proc. of the 13th European Wave and Tidal Energy Conference*, Naples, Italy, 1st to 6th september, 2019.
22. Thiébot J., P. Bailly du Bois, S. Guillou. 2015. Numerical modeling of the effect of tidal stream turbines on the hydrodynamics and the sediment transport – Application to the Alderney Race (Raz Blanchard), France. *Renewable Energy*, **Vol. 75**, pp. 356-365.
23. Furgerot L., P. Bailly du Bois, Y. Méar, M. Morillon, E. Poizot, A.-C. Bennis. 2018. Velocity profile variability at a tidal-stream energy site (Alderney Race, France): from short (second) to yearly time scales. *Proc. of OCEANS 2018*, Kobe, Japan.
24. Egbert G.D., S.Y. Erofeeva, R.D. Ray. 2010. Assimilation of altimetry data for nonlinear shallow-water tides: quarter-diurnal tides of the Northwest European Shelf. *Cont. Shelf Res.*, **Vol. 30**, pp. 668-679.
25. Lazure P., F. Dumas. 2008. An external–internal mode coupling for a 3D hydrodynamical model for applications at regional scale (MARS). *Advances in Water Resources*, **Vol. 31(2)**, pp. 233-250.
26. Le Roy R., B. Simon. 2003. Réalisation et validation d'un modèle de marée en Manche et dans le Golfe de Gascogne. Application à la réalisation d'un nouveau programme de réduction des sondages bathymétriques. Technical Report 002/03. Service Hydrographique et Océanographique de la Marine.
27. Vinod A., A. Banerjee. 2019. Performance and near-wake characterization of a tidal current turbine in elevated levels of free stream turbulence. *Applied Energy*, **Vol. 254**, 17 p.

28. Thiébot J., S. Guillou, V.T. Nguyen. 2016. Modelling the effect of large arrays of tidal turbines with depth-averaged Actuator Disks. *Ocean Engineering*, **Vol. 126**, pp. 265-275.
29. Togneri M., M. Lewis, S.P. Neill, I. Masters. 2017. Comparison of ADCP observations and 3D model simulations of turbulence at a tidal energy site. *Renewable Energy*, **Vol. 114A**, pp. 273-282.
30. Bourgoin A. 2019. Bathymetry induced turbulence modelling the Alderney Race site: regional approach with TELEMAC-LES. PhD thesis. University of Caen. https://tel.archives-ouvertes.fr/tel-02310681. 171 p.
31. Bourgoin A., S.S. Guillou, J. Thiébot, R. Ata. Accepted. Turbulence characterization at a tidal energy site using Large Eddy Simulations: Case of the Alderney Race. *Theme issue of Philosophical Transactions A.*
32. Bourgoin A., S.S. Guillou, J. Thiébot., R. Ata. 2020. Use of Large-Eddy Simulation for the bed shear stress estimation over a dune. *International Journal of Sediment Research*. https://doi.org/10.1016/j.ijsrc.2019.10.002.
33. Mercier P., M. Grondeau, S.S. Guillou, J. Thiébot, E. Poizot. 2019. High resolution large eddy simulation for tidal site turbulence characterization. *13th European Wave and Tidal Energy Conference Proceeding*, Napoli, Italy.
34. Mercier P., M. Grondeau, S. Guillou, J. Thiébot, E. Poizot. 2020. Numerical study of the turbulent eddies generated by the seabed roughness. Case study at a tidal power site. *Applied Ocean Research*, **Vol. 97, 8p.**
35. Mercier P., M. Ikhennicheu, S.S. Guillou, G. Germain, E. Poizot, M. Grondeau, J. Thiébot, P. Druault. 2020. The merging of Kelvin–Helmholtz vortices into large coherent flow structures in a high Reynolds number flow past a wall-mounted square cylinder. *Ocean Engineering*, **Vol. 204**, 13p.
36. Thiébaut M., J.-F. Filipot, C. Maisondieu, G. Damblans, R.Duarte, E. Droniou, N. Chaplain, S. Guillou. 2019. A comprehensive assessment of turbulence at a tidal-stream energy site influenced by wind-generated ocean waves. *Energy*. https://doi.org/10.1016/j.energy.2019.116550.
37. Thiébaut M., J.-F. Filipot, C. Maisondieu, G. Damblans, A. Peterse, R. Duarte, E. Droniou, N. Chaplain, S.S. Guillou. Accepted. Assessing the turbulent kinetic energy budget in an energetic tidal flow from coupled ADCPs measurements. *Theme issue of Philosophical Transactions A*.
38. Thiébaut M., J.-F. Filipot, C. Maisondieu, G. Damblans, C. Jochum, L.F. Kilcher, N. Chaplain, S.S. Guillou. Accepted. Characterization of the vertical evolution of the 3D turbulence for fatigue design of tidal turbines. *Theme issue of Philosophical Transactions A*.
39. Petersen M.R., M. W. Hecht, and B. A. Wingate. 2008. Efficient form of the lans-alpha turbulence model in a primitive-equation ocean model. *Journal of Computational Physics*, **Vol. 227(11)**, pp. 5717 – 5735.
40. Hecht M.W., D. D. Holm, M. R. Petersen, and B. A. Wingate. 2008. Implementation of the lans-alpha turbulence model in a primitive equation ocean model. *Journal of Computational Physics*, **Vol. 227(11)**, pp. 5691 – 5716.
41. Guillou N., G. Chapalain G., S.P. Neill. 2016. The influence of waves on the tidal kinetic energy resource at a tidal stream energy site. *Applied Energy*, **Vol. 180**, pp. 402-415.
42. Benoit M., F. Lafon. 2004. A nearshore wave atlas along the coasts of France based on the numerical modeling of wave climate over 25 years. *Proc. 29th Int. Conf. on Coastal Eng. (ICCE2004)*, Lisbon, Portugal. https://doi.org/10.1142/9789812701916_0057.
43. Charles E., D. Idier, J. Thiébot, G. Le Cozannet, R. Pedreros, F. Ardhuin, S. Planton. 2012. Present wave climate in the bay of biscay: Spatiotemporal variability and trends from 1958 to 2001. *Journal of Climate*, **Vol. 25(6)**, pp. 2020-2039.
44. Boudière E., C. Maisondieu, F. Ardhuin, M. Accensi, J. Lepesqueur. 2013. A suitable metocean hindcast database for the design of Marine energy converters. *International Journal of Marine Energy*, **Vol. 3–4**, pp. 40-52.

45. Guillou N. 2014. Wave-energy dissipation by bottom friction in the English Channel. *Ocean Engineering*, Elsevier, **Vol. 82**, pp.42 - 51.
46. Tolman H.L. 2014. User Manual and System Documentation of WAVEWATCH-IIITM Version 4.18. Technical Report, NOAA/NWS/NCEP/MMAB/.
47. Saha S. and coauthors. 2010. The NCEP Climate Forecast System Reanalysis. *Bull. Amer. Meteor. Soc.*, **Vol. 91**, pp. 1015–1057.
48. Saha S. and coauthors. 2014. The NCEP Climate Forecast System Version 2. *J. Climate*, **Vol. 27**, pp. 2185-2208.
49. Accensi M., C. Maisondieu. 2015. HOMERE. Ifremer - Laboratoire Comportement des Structures en Mer. https://doi.org/10.12770/cf47e08d-1455-4254-955e-d66225c9dc90.
50. Bennis A.-C., P. Bailly du Bois, F. Dumas, C. Lathuillère, F. Adong, J.-F. Filipot. 2018. Towards a realistic modelling of wave-current-turbulence interactions in Alderney Race. *Proceeding of OTO'18/OCEANS'18 MTS/IEEE*, Kobe, Japan.
51. MeyGen Ltd. 2018. Lessons learnt from MeyGen Phase 1a Part 2/3: Construction Phase. 23p.
52. Black and Veatch. 2005. UK tidal stream energy resource assessment, Commissioned by the Carbon Trust. pp. 10-31.
53. Owen A. 2005. Tidal stream resource assessment for the channel islands area, Report for Black and Veatch Consulting Ltd.
54. Black and Veatch. 2011. UK tidal current resource and economics. Commissioned by the Carbon Trust and npower, Project number 121393.
55. Garrett C., P. Cummins. 2005. The power potential of tidal currents in channels, *R. Soc. A*, **Vol. 461**, pp. 2563–2572.
56. Energy Technology Support Unit. 1993. Tidal Stream Energy Review, Technical report ETSUT/05/00155/REP, Harwell Laboratory.
57. European Commission. 1996. The exploitation of tidal marine currents, Wave Energy, Project results. Technical Report EUR 16683 EN, 1996.
58. Bahaj A. S. and L. Myers. 2004. Analytical estimates of the energy yield potential from the Alderney Race (Channel Islands) using marine current energy converters. *Renewable Energy*, **Vol. 29(12)**, pp. 1931-1945.
59. Myers L., A. S. Bahaj. 2005. Simulated electrical power potential harnessed by marine current turbine arrays in the Alderney Race. *Renewable Energy*, **Vol. 30(11)**, pp. 1713-1731.
60. Coles D.S., L.S. Blunden, A.S. Bahaj. Accepted. The energy yield potential of a large tidal stream turbine array in the Alderney Race. *Theme issue of Philosophical Transactions A*.
61. Pinon G., M. Fernández Hurst, E. Lukeba. 2017. Semi-analytical estimate of energy production from a tidal turbine farm with the account of ambient turbulence. *International Journal of Marine Energy*, **Vol. 19**, pp. 70-82.
62. Mycek P., B. Gaurier, G. Germain, G. Pinon, E. Rivoalen. 2014. Experimental study of the turbulence intensity effects on marine current turbines behaviour. part I: One single turbine. *Renewable Energy*, **Vol. 66**, pp. 729-746.
63. Mycek P., B. Gaurier, G. Germain, G. Pinon, E. Rivoalen. 2014. Experimental study of the turbulence intensity effects on marine current turbines behaviour. part II: two interacting turbines. *Renewable Energy*, **Vol. 68**, pp. 876-892.
64. Neill S.P., E.J. Litt, S.J. Couch, A.G. Davies. 2009. The impact of tidal stream turbines on large-scale sediment dynamics. *Renewable Energy*, **Vol. 34(12)**, pp. 2803-2812.
65. Fairley I., I. Masters, H. Karunarathna. 2015. The cumulative impact of tidal stream turbine arrays on sediment transport in the Pentland Firth. *Renewable Energy*, **Vol. 80**, pp. 755-769.

66. Martin-Short R., J. Hill, S. C. Kramer, A. Avdis, M. D. Piggott. 2015. Tidal resource extraction in the Pentland Firth, UK: Potential impacts on flow regime and sediment transport in the Inner Sound of Stroma. *Renewable Energy*, **Vol. 76**, pp. 596-607.
67. Kresning B., M. Reza. Hashemi, S.P. Neill, J. A. Mattias Green, H. Xue. 2019. The impacts of tidal energy development and sea-level rise in the Gulf of Maine. *Energy*, **Vol. 187**, Article 115942. 13p.
68. Guillou N., J. Thiébot, G. Chapalain. 2019. Turbines' effects on water renewal within a marine tidal stream energy site. *Energy*, **Vol.189**, Article 116113. 10p.
69. Soulsby R.L. 1997. Dynamics of marine sands. HR Wallingford. Tech. Rep. SR 466.
70. Van Rijn L.C. 1984. Sediment transport: part I: bed load transport. *J Hydraul Div*, **Vol. 110**, pp. 1431-1456.
71. Van Rijn L.C. 1984. Sediment transport: part II: suspended load transport. *J Hydraul Div*, **Vol. 110**, pp. 1613-1641.
72. Blunden L.S., S.G. Haynes, A.S. Bahaj. 2018. Dynamic sandbanks in close proximity to sites of interest for tidal current power extraction. *The 4th Asian Wave and Tidal Energy Conference*, Taipei, Taiwan. 6 p.
73. Vennell R., S.W. Funke, S. Draper, C. Stevens, T. Divett. 2015. Designing large arrays of tidal turbines: A synthesis and review. *Renewable and Sustainable Energy Reviews*, **Vol. 41**, pp. 454-472.
74. Coles D.S., S.C. Kramer, M.D. Piggott, A. Advis, A. Angeloudis. 2017. Optimisation of tidal stream turbine arrays within the Alderney Race. *Proceedings of the 12th European Wave and Tidal Energy Conference, Cork, Ireland*. 10 p.
75. Goss Z.L., M.D. Piggott, S.C. Kramer, A. Avdis, A. Angeloudis, C.J. Cotter. 2018. Competition effects between nearby tidal turbine arrays - optimal design for Alderney Race. *Advances in Renewable Energies Offshore*. Editor: C. Guedes Soares. Taylor and Francis. pp. 255 - 264.
76. Funke S.W., S. C. Kramer, M. D. Piggott. 2016. Design optimisation and resource assessment for tidal-stream renewable energy farms using a new continuous turbine approach. *Renewable Energy*, **Vol. 99**, pp. 1046-1061.
77. Lo Brutto O.A., J. Thiébot, S.S. Guillou, H. Gualous. 2016. A semi-analytic method to optimize tidal farm layouts – Application to the Alderney Race (Raz Blanchard), France. *Applied Energy*, **Vol. 183**, pp. 1168-1180.
78. Jensen N.O. 1983. A Note on Wind Generator Interaction. Tech. rep., Risø National Laboratory, Riso-M-2411, Roskilde, Denmark. 16 p.
79. Katic I., J. Højstrup, N.O. Jensen. 1986. A simple model for cluster efficiency. *European Wind Energy Association Conference and Exhibition*, pp. 407-410.
80. Barthelmie R.J., S.C. Pryor, S.T. Frandsen, K.S. Hansen, J. Schepers, K. Rados, W. Schlez, A. Neubert, L. Jensen, S. Neckelmann. 2010. Quantifying the impact of wind turbine wakes on power output at offshore wind farms. *J. Atmos. Ocean. Technol.*, **Vol. 27 (8)**, pp. 1302-1317.
81. Lo Brutto O.A., V.T. Nguyen, S.S. Guillou, J. Thiébot, H. Gualous. 2016. Tidal farm analysis using an analytical model for the flow velocity prediction in the wake of a tidal turbine with small diameter to depth ratio. *Renewable Energy*, **Vol. 99**, pp. 347-359.
82. Nguyen V.T., A. Santa Cruz, S.S. Guillou, M.N. Shiekh Elsouk, J. Thiébot. 2019. Effects of the Current Direction on the Energy Production of a Tidal Farm: The Case of Raz Blanchard (France). *Energies*. **Vol. 12(13)**, 2478. 20 p.
83. Zanforlin S. 2018. Advantages of vertical axis tidal turbines set in close proximity: A comparative CFD investigation in the English Channel. *Ocean Engineering*. **Vol. 156**, pp. 358-372.
84. Nguyen V.T., S.S. Guillou, J. Thiébot, A. Santa Cruz. 2016. Modelling turbulence with an Actuator Disk representing a tidal turbine. *Renewable Energy*, **Vol. 97**, pp. 625-635.
85. Lopez G., A.-C. Bennis, Y. Barbin, L. Benoit, R. Cambra, D.C. Conley, J-L. Lagarde, L. Marié, L. Perez, S. Smet, L. Wyatt. 2018. Hydrodynamics of Raz Blanchard: HF radar wave measurements. *Proceeding of ICOE 2018*, Cherbourg, France.

86. Lopez G., A.-C. Bennis, Y. Barbin, L. Benoit, R. Cambra, D.C. Conley, L. Marié, L. Perez, A. Sentchev, L. Wyatt. 2019. Surface hydrodynamics of the Alderney Race from HF Radar Measurements. *Proceeding of EWTEC 2019*, Naples, Italy.
87. Thiébot J., S.S. Guillou, E. Droniou. 2020. Influence of the 18.6-year lunar nodal cycle on the tidal resource of the Alderney Race, France. *Applied Ocean Research.* **Vol. 97**. Article 102107.

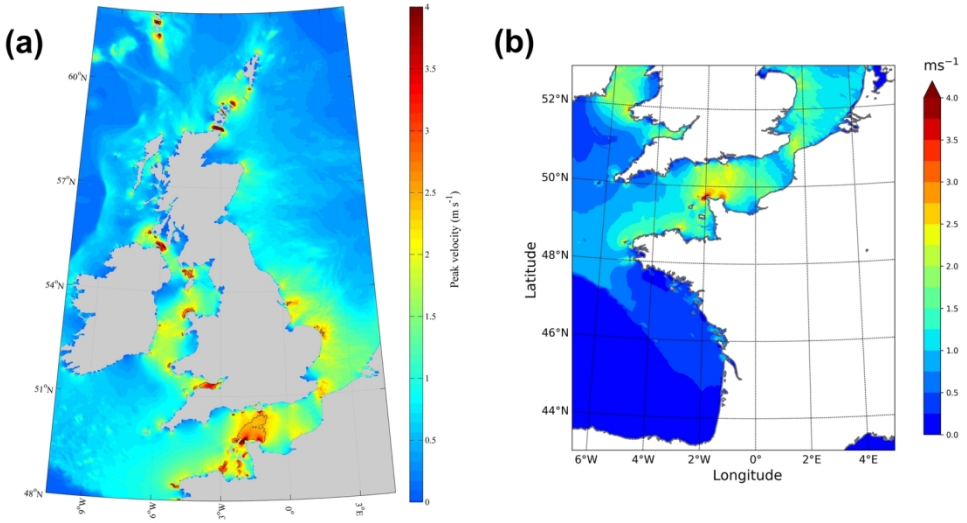

Spatial coverage of the models of (a) [10] and (b) [12]. The colour represents the maximum depth-averaged tidal velocity magnitude. The velocities have been computed from the (a) M2, S2, K1, O1 and M4 constituents and (b) M2, S2, N2, K2, K1, O1, P1, Q1, M4 and MS4 constituents. Figure 1a was reprinted from [10] Robins et al. (2015) Characterising the spatial and temporal variability of the tidal-stream energy resource over the northwest European shelf seas. Applied Energy, Vol. 147, pp. 510-522. Copyright 2020, with permission from Elsevier. Figure 1b was adapted from [12] Guillou et al. (2018) Characterising the tidal stream power resource around France using a high-resolution harmonic database. Renewable Energy, Vol. 123, pp. 706-718. Copyright 2020, with permission from Elsevier.

152x82mm (300 x 300 DPI)

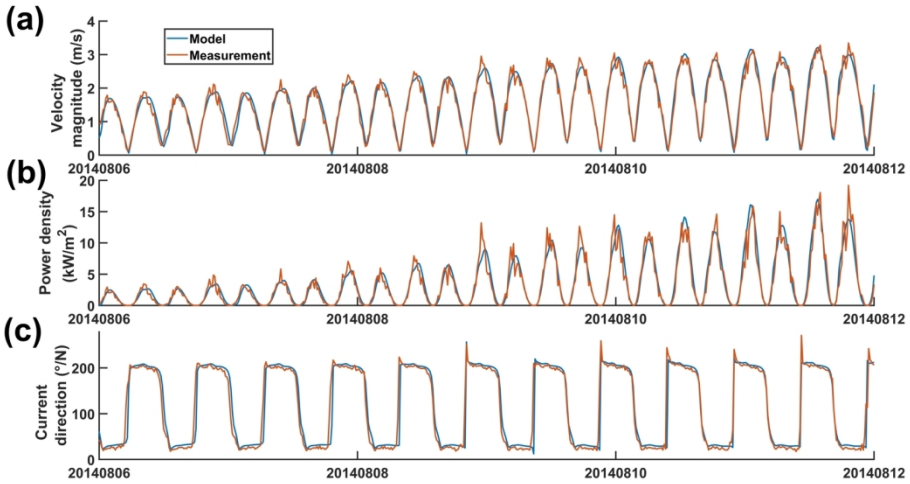

Time-series of horizontal current magnitude (a), power density (b) and current direction at hub height (c). The blue curve represents model predictions. The red curve represents measurements by ADCP. The time-series were extracted 15 m above the seabed. Reprinted from [20] Thiébot et al. (2020) Wake field study of tidal turbines under realistic flow conditions. Renewable Energy, ttps://doi.org/10.1016/j.renene.2019.11.129. Copyright 2020, with permission from Elsevier.

152x77mm (300 x 300 DPI)

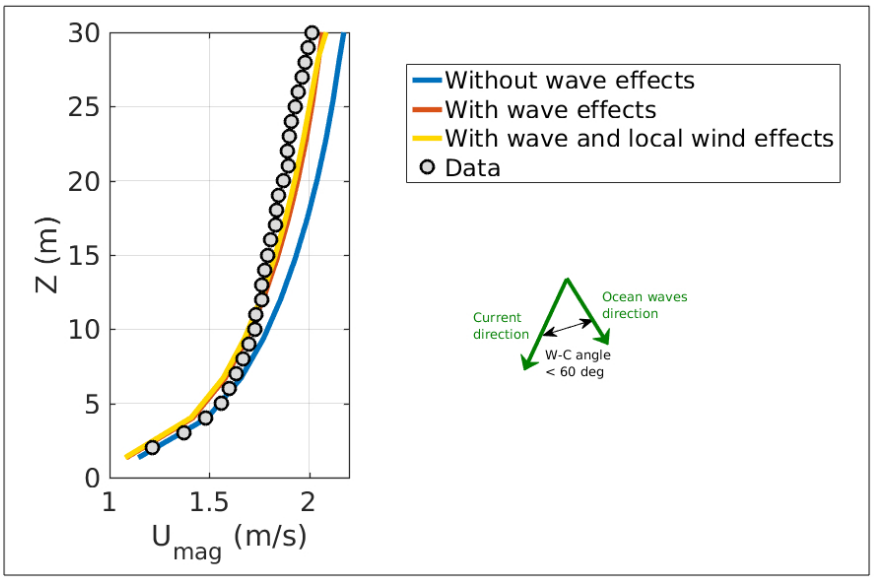

Vertical profiles of tidal current speed (November, the 25th, in 2017, 17:00). The wave conditions were such that Hs (the significant wave height) = 1.6 m, Tp (the peak period) = 6 s and Dp (the peak direction) = 320°/North. Measurements are represented with grey-black circles and numerical results are represented with solid lines (blue line: run without waves, red line: run with wave effects and yellow line: run with wave and local wind effects). This figure has been adapted from [19].

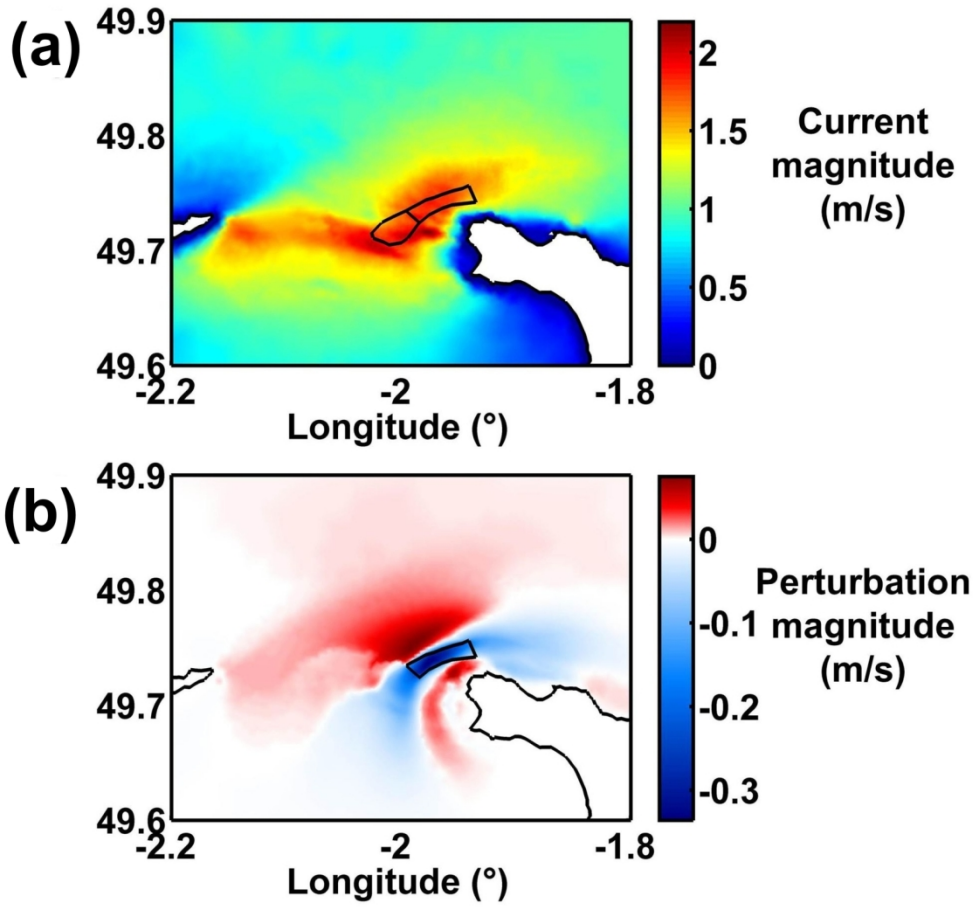

Impact of a 290 MW array on the mean current velocity magnitude: (a) baseline; (b) changes induced by a tidal farm. The results are averaged over a 1-month-long simulation. Reprinted from [22] Thiébot et al. (2015) Numerical modelling of the effect of tidal stream turbines on the hydrodynamics and the sediment transport – Application to the Alderney Race (Raz Blanchard), France. Renewable Energy, Vol. 75, pp. 356-365. Copyright 2020, with permission from Elsevier.

152x141mm (300 x 300 DPI)

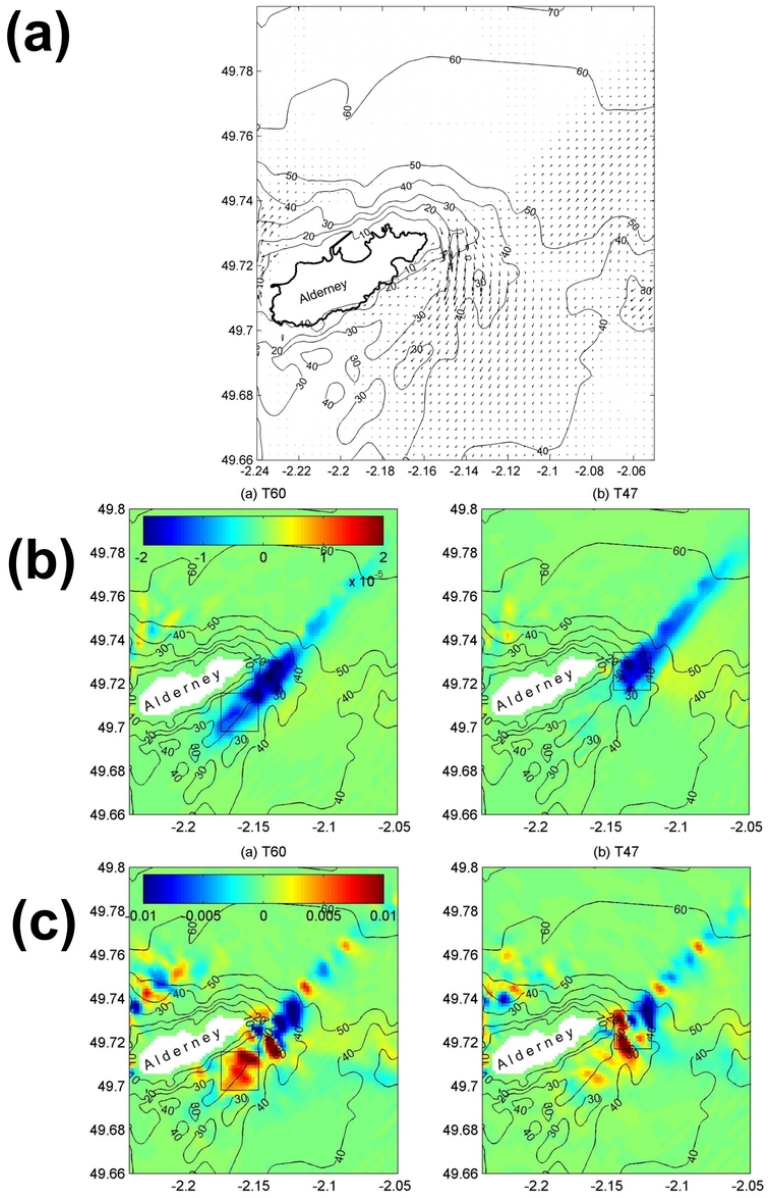

(a) Residual sediment transport. (b) Change in the volumetric sediment transport rate (in m2s−1) due to energy extraction, averaged over a spring-neap cycle. (c) Change in bed level (in m) due to energy extraction, averaged over a spring-neap cycle. The boxes show the limits of the array. Reprinted from [17] Neill et al. (2012) Impact of tidal energy converter (TEC) arrays on the dynamics of headland sand banks. Renewable energy, Vol 37, n°1, pp. 387-397. Copyright 2020, with permission from Elsevier.

63x99mm (300 x 300 DPI)

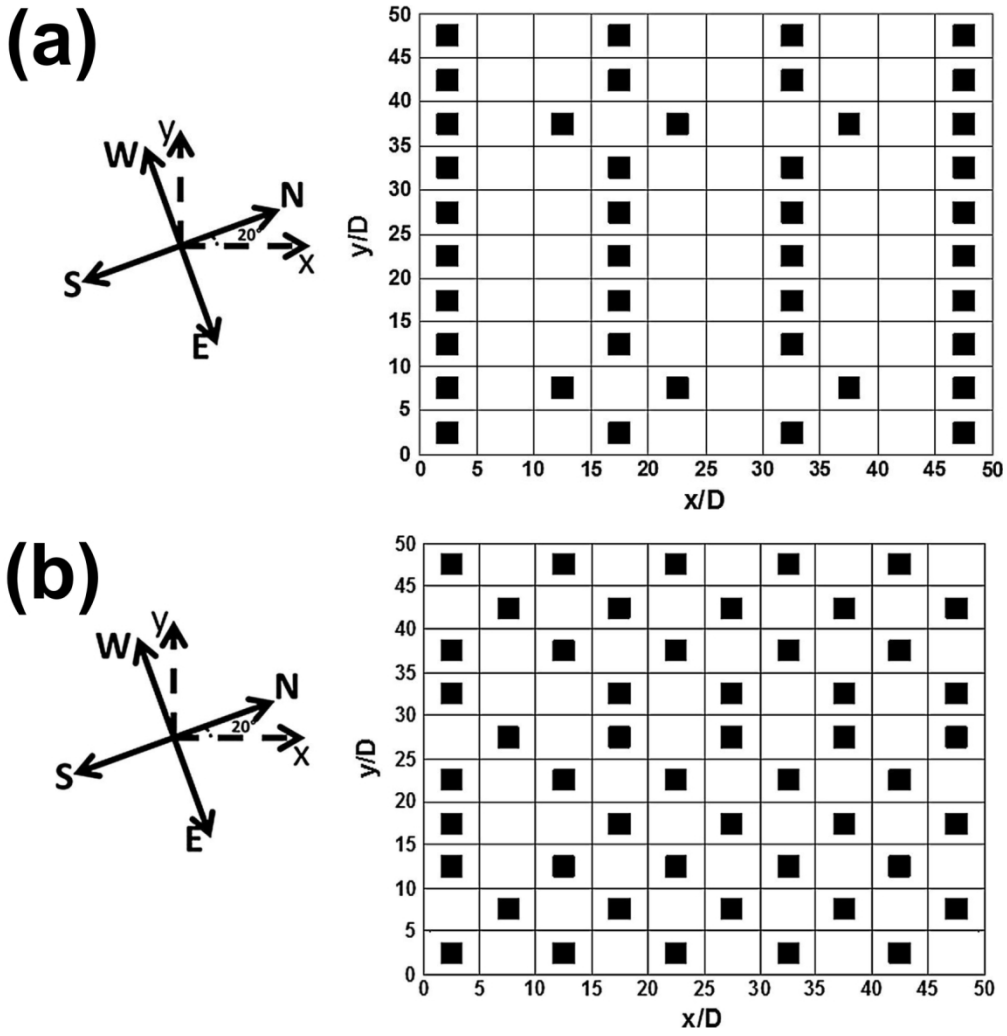

Influence of the current misalignment on the optimal tidal array layout. Optimal layout obtained with the hydrodynamic data of the Alderney with bidirectional flows (a), and with misalignment between ebb and flood phases of the tidal cycle (b). The predominant current direction is parallel to the x-axis. Reprinted from [77] Lo Brutto et al. (2016) A semi-analytic method to optimize tidal farm layouts – Application to the Alderney Race (Raz Blanchard), France. Applied Energy. Volume 183, Pages 1168-1180. Copyright 2020, with permission from Elsevier.

145x152mm (300 x 300 DPI)

References	Model	Studied zone / Minimum cell size	Forcing	Data used for the model calibration/ validation	Objectives
DTI [8]	POLCOMS (FD)	1.8 km	Not mentioned	Not mentioned	Resource assessment (intercomparison of sites)
SHOM [9]	HYCOM3D (FD)	1.8 km	Operational Mercator global ocean analysis and forecast system + wind + atmospheric pressure	Not mentioned	Resource assessment (intercomparison of sites)
Robins et al. [10]	ROMS3D (FD)	NW European continental shelf / 1 km	10 constituents (TPXO7)	Tidal gauges (20 stations) + Current meters (15 stations)	Resource assessment (intercomparison of sites)
Campbell et al. [11]	MARS2D (FD)	Coasts of France / 250 m	115 constituents cstFRANCE) + wind + atmospheric pressure	Tidal gauges (19 stations)	Resource assessment (intercomparison of sites)
Guillou et al. [12]	Harmonic database built from MARS2D (FD) predictions	Coasts of France / 250 m	115 constituents (cstFRANCE) + wind + atmospheric pressure	Tidal gauges (18 stations) + Current meters (40 stations)	Resource assessment (intercomparison of sites)
Bailly du Bois et al. [13]	MARS2D (FD)	NW European continental shelf / 110 m	10 constituents (FES2004) + wind + atmospheric pressure	Current meters (11 stations) + Tidal gauges (3 stations) + Tracer releases + Drifter tracking	Dispersion of solute tracers
Thiébaut et al. [14]	MARS2D (FD)	NW European continental shelf / 110 m	14 constituents FES2012	Same as Bailly du Bois et al. (2012) + Towed and bottom-mounted current meters	Resource assessment
Pal et al. [15]	ADCIRC (FE)	English Channel / min. cell size not mentioned	8 constituents	Not mentioned	Resource assessment
Blunden et al. [16]	Telemac2D (FE)	English Channel /1 km	Tidal constituents interpolated between two harbours	Tidal gauges (14 stations)	Resource assessment (model validation)
Neill et al. [17]	POLCOMS3D (FD)	Alderney Race and surrounding waters / 500 m	2 constituents [18]	Tidal gauges (3 stations) + Admiralty tidal diamonds (4 stations)	Effect of the tidal energy extraction
Coles et al. [1]	Telemac2D (FE)	English	9 constituents	Tidal gauges (13	Resource

		Channel / 250 m		stations) + Current meters (3 stations)	assessment + Effect of the tidal energy extraction
Bennis et al. [19]	MARS3D (FD) coupled to WaveWatch-III	Western part of the English Channel / 120 m	115 tidal constituents (cstFRANCE) + Waves + Winds	Tidal gauges (2 stations) + ADCP (waves and currents) at 1 station	Interactions between waves and current
Thiébot et al. [20]	Telemac3D (FE)	English Channel / 100 m	11 constituents TPXO8	Current meters (5 stations)	Wake-field study

Reference	[82]	[20]
3D Solver	ANSYS Fluent	Telemac3D
Model settings	Steady RANS equations Finite Volume Turbulence model : k-ε Hexahedral elements	Unsteady RANS equations Finite Element Turbulence model : k-ε Prismatic elements (triangular cell extruded over the vertical using σ-layers)
Domain size	Restricted to the area occupied by the array (680 m x 804 m)	English Channel with refinement in the area occupied by the array
Tested layout	9 aligned turbines (3 rows), 10 staggered turbines (3 rows)	Isolated turbine, 4 staggered layouts, 4 aligned layouts (with different spacings between devices)
Hydrodynamic conditions	Current data representative of different times of a mean tide. Rectilinear flow and misalignment between ebb and flood flow.	1 spring tide. Realistic tidal conditions (3D model forced validated with ADCP data).